Neuropsychopharmacology (2012) 37, 1338–1356

www.neuropsychopharmacology.org

Increased Kv1 Channel Expression May Contribute to Decreased sIPSC Frequency Following Chronic Inhibition of NR2B-Containing NMDAR

Shuijin He[1,2], Li-Rong Shao[1], W Bradley Rittase[1] and Suzanne B Bausch*[,1,2]

[1]Department of Pharmacology, Uniformed Services University School of Medicine, Bethesda, MD, USA; [2]Graduate Program in Neuroscience, Uniformed Services University School of Medicine, Bethesda, MD, USA

Numerous studies have documented the effects of chronic *N*-methyl-D-aspartate receptor (NMDAR) blockade on excitatory circuits, but the effects on inhibitory circuitry are not well studied. NR2A- and NR2B-containing NMDARs play differential roles in physiological processes, but the consequences of chronic NR2A- or NR2B-containing NMDAR inhibition on glutamatergic and GABAergic neurotransmission are unknown. We investigated altered GABAergic neurotransmission in dentate granule cells and interneurons following chronic treatment with the NR2B-selective antagonist, Ro25,6981, the NR2A-prefering antagonist, NVP-AAM077, or the non-subunit-selective NMDAR antagonist, D-APV, in organotypic hippocampal slice cultures. Electrophysiological recordings revealed large reductions in spontaneous inhibitory postsynaptic current (sIPSC) frequency in both granule cells and interneurons following chronic Ro25,6981 treatment, which was associated with minimally altered sIPSC amplitude, miniature inhibitory postsynaptic current (mIPSC) frequency, and mIPSC amplitude, suggesting diminished action potential-dependent GABA release. Chronic NVP-AAM077 or D-APV treatment had little effect on these measures. Reduced sIPSC frequency did not arise from downregulated $GABA_AR$, altered excitatory or inhibitory drive to interneurons, altered interneuron membrane properties, increased failure rate, decreased action potential-dependent release probability, or mGluR/$GABA_B$ receptor modulation of GABA release. However, chronic Ro25,6981-mediated reductions in sIPSC frequency were occluded by the K^+ channel blockers, dendrotoxin, margatoxin, and agitoxin, but not dendrotoxin-K or XE991. Immunohistochemistry also showed increased Kv1.2, Kv1.3, and Kv1.6 in the dentate molecular layer following chronic Ro25,6981 treatment. Our findings suggest that increased Kv1 channel expression/function contributed to diminished action potential-dependent GABA release following chronic NR2B-containing NMDAR inhibition and that these Kv1 channels may be heteromeric complexes containing Kv1.2, Kv1.3, and Kv1.6.
Neuropsychopharmacology (2012) **37,** 1338–1356; doi:10.1038/npp.2011.320; published online 4 January 2012

Keywords: hippocampus; interneuron; plasticity; slice culture; dentate granule cell; potassium channel

INTRODUCTION

The *N*-methyl-D-aspartate receptors (NMDARs) are heteromeric ionotropic glutamate receptors composed of NR1 and NR2A-D, with NR2A and NR2B being the predominant NR2 subunits in hippocampus and cortex (Monyer *et al*, 1994; Yamakura and Shimoji, 1999). NMDAR activation plays a crucial role in physiological brain processes, including neuronal survival (Ikonomidou *et al*, 1999) and synaptic plasticity (Dingledine *et al*, 1999; Mori and Mishina, 1995). Chronic NMDAR blockade increases synaptic reorganization in glutamatergic circuits, presynaptic glutamate release, and postsynaptic glutamate receptor clustering (Bausch *et al*, 2006; Bear *et al*, 1990; Cline *et al*, 1987; Lin and Constantine-Paton, 1998; McKinney *et al*, 1999; O'Brien *et al*, 1998; Rao and Craig, 1997). Such changes increase neuronal excitability and may exacerbate electrographic seizures following chronic NMDAR blockade (Bausch *et al*, 2006).

NMDARs are also highly expressed in hippocampal interneurons (Monyer *et al*, 1994; Moriyoshi *et al*, 1991), where they regulate inhibitory synapse plasticity (Lu *et al*, 2000; Ouardouz and Sastry, 2000; Xie and Lewis, 1995), postsynaptic $GABA_A$ receptor ($GABA_AR$) membrane insertion (Marsden *et al*, 2007; Xie and Lewis, 1995), and presynaptic GABA release (Drejer *et al*, 1987; Pin *et al*, 1988). Chronic NMDAR blockade alters $GABA_AR$ subunit expression (Matthews *et al*, 2000) and slightly reduces miniature inhibitory postsynaptic currents (mIPSCs) (Bausch *et al*, 2006) but, overall, documentation of the effects of chronic NMDAR blockade on inhibitory interneurons lags far behind that for excitatory circuits.

*Correspondence: Dr SB Bausch, Department of Pharmacology, Uniformed Services University School of Medicine, Room C2007, 4301 Jones Bridge Road, Bethesda, MD 20814-4799, USA, Tel: +1 301 295 3226, Fax: +1 301 295 3220, E-mail: sbausch@usuhs.mil
Received 26 July 2011; revised 21 October 2011; accepted 29 November 2011

NR2A- and NR2B-containing NMDARs differ in subcellular localization, trafficking, biophysical properties, and roles in physiological processes (Barria and Malinow, 2002; Flint *et al*, 1997; Lavezzari *et al*, 2004; Monyer *et al*, 1994). Activation of NR2A-containing NMDARs promotes neuronal survival, whereas activation of NR2B-containing NMDARs increases neuronal death (Hardingham *et al*, 2002). Opposing roles of NR2A- and NR2B-containing NMDARs in synaptic plasticity induction have also been reported (Liu *et al*, 2004), but these findings remain controversial because others showed a requirement for both NR2A- and NR2B-containing NMDARs (Barria and Malinow, 2005; Berberich *et al*, 2005; Morishita *et al*, 2007; Tang *et al*, 1999; Weitlauf *et al*, 2005). Finally, chronic inhibition of NR2B-containing NMDARs dramatically reduced whereas chronic inhibition of NR2A-containing NMDARs did not significantly affect subsequent electrographic seizures in organotypic hippocampal slice cultures (Dong and Bausch, 2005; Wang and Bausch, 2006). The effects of selective chronic inhibition of NR2A- and NR2B-containing NMDARs on excitatory and inhibitory circuits are unknown. Documenting these effects is critical given the status of NR2B-selective antagonists in clinical trials for major depression, pain, and Parkinson's disease (Mony *et al*, 2009; www.clinicaltrials.gov) and the need for a greater understanding of the contribution of NR2A- and NR2B-containing NMDARs in physiological processes. In this study, we examined the changes in $GABA_A$R-mediated neurotransmission because GABAergic transmission can influence seizure expression, major depression, pain, and Parkinson's disease, and the effects of chronic NMDAR inhibition on GABAergic transmission are largely unknown. Based upon our previous findings, we hypothesized that chronic inhibition of NR2B-containing NMDARs would enhance whereas chronic inhibition of NR2A-containing NMDARs would not dramatically affect $GABA_A$R-mediated transmission.

Representative NMDAR antagonists were selected based on their pharmacological properties as described previously (Wang and Bausch, 2004). The frequently used NR2B-specific antagonist, Ro25,6981 (1 μM), was selected because of its high affinity and specificity for NR2B-containing NMDARs (Fischer *et al*, 1997; Smith and McMahon, 2006; Zhao *et al*, 2005; Zhou and Baudry, 2006), and our previous concentration-response study showed a maximal effect of Ro25,6981 on seizure expression at 1 μM (Dong and Bausch, 2005). Although chronic inhibition of NR2B-containing NMDARs with either Ro25,6981 or ifenprodil dramatically reduced electrographic seizures in our previous study (Wang and Bausch, 2004), we chose Ro25,6981 over ifenprodil for the current study because of possible interactions of ifenprodil with α-adrenergic receptors, serotonin receptors, and calcium channels (Chenard *et al*, 1995; Church *et al*, 1994; McCool and Lovinger, 1995). The NR2A-selective antagonist, NVP-AAM077 (50 nM), was chosen because of its high preference for NR2A-containing NMDARs at this concentration (Auberson *et al*, 2002; Feng *et al*, 2004; Neyton and Paoletti, 2006) and frequent use in studies documenting differential NR2A/NR2B effects (Massey *et al*, 2004; Zhou and Baudry, 2006). D(−)-2-amino-5-phosphonopentanoic acid (D-APV, 50 μM) was included because of its high NMDAR specificity and to facilitate comparison with previous physiological and homeostatic plasticity studies.

MATERIALS AND METHODS

Organotypic Hippocampal Slice Cultures

Slice cultures were prepared using the interface method (Stoppini *et al*, 1991) as described previously (Bausch *et al*, 2006). Briefly, postnatal day 10–11 Sprague-Dawley rats (Taconic, Germantown, NY) were anesthetized with pentobarbital and decapitated. Brains were removed and cut into 400 μm transverse sections using a McIlwain tissue chopper. Hippocampal slices were separated from entorhinal cortex in Gey's balanced salt solution (GBSS) composed of (in mM) 137 NaCl, 5 KCl, 0.25 $MgSO_4$, 1.5 $CaCl_2$, 1.05 $MgCl_2$, 0.84 Na_2HPO_4, 0.22 K_2HPO_4, 2.7 $NaHCO_3$, and 41.6 glucose. The middle 4–6 slices of each hippocampus were placed onto tissue culture membrane inserts (Millipore, Bedford, MA) in a culture dish with medium consisting of 50% minimum essential medium, 25% Hank's buffered salt solution, 25% heat-inactivated horse serum, 0.5% GlutaMax, 10 mM HEPES (all from Invitrogen, Carlsbad, CA), and 6.5 mg/ml glucose (pH 7.2). Cultures were maintained at 37 °C under room air + 5% CO_2 and medium was changed three times per week. Cultures were treated with D-APV (50 μM; Tocris Cookson, Ellisville, MO), Ro25,6981 hydrochloride (1 μM; Sigma), or NVP-AAM077 (50 nM; Dr Yves Auberson, Novartis Institutes for Biomedical Research, Basel, Switzerland) diluted in medium for the entire 17–21 DIV culture period. Vehicle-treated cultures were treated similarly, but drugs were omitted. Experiments in vehicle- and NMDAR antagonist-treated cultures were conducted concurrently under identical conditions. Only cultures showing bright, well-defined cell layers were included.

Electrophysiological Recordings

Recordings were conducted as described previously (Bausch *et al*, 2006) in dentate granule cells and interneurons at the dentate granule cell layer/hilus border (D/H border interneurons). Briefly, the membrane containing a single cultured slice was cut and transferred to a submerged recording chamber mounted onto a Zeiss Axioskop microscope with IR-DIC optics (Carl Zeiss, Thornwood, NY). Slice cultures were superfused (2–3 ml/min) continuously with artificial cerebrospinal fluid (aCSF) composed of (in mM) 124 NaCl, 4.9 KCl, 1.2 KH_2PO_4 2.4 $MgSO_4$, 2.5 $CaCl_2$, 25.6 $NaHCO_3$, and 10 glucose equilibrated with 95% O_2 and 5% CO_2. Tetrodotoxin (TTX, 1 μM; Sigma), D-APV (50 μM), bicuculline methiodide (BMI, 10 μM; Tocris Cookson), 6-cyano-7-nitroquinoxaline-2,3-dione (CNQX, 10 μM; Tocris Cookson), 4-aminopyridine (4-AP; Acros Organics, Pittsburgh, PA), tetraethylammonium (TEA; Sigma), (2S)-[[(1S)-1-(3,4-dichlorophenyl)ethyl] amino-2-hydroxypropyl](phenylmethyl)phosphinic acid (CGP55845, 3 μM; Tocris Cookson), RS-α-cyclopropyl-4-phosphophenylglycine (CPPG, 200 μM; Tocris Cookson), dendrotoxin (200 nM; Sigma), dendrotoxin-K (100 nM; Sigma), margatoxin (10 nM; Sigma), and 10,10-bis(4-pyridinylmethyl)-9(10*H*)-anthracenone dihydrochloride (XE 991, 10 μM; Tocris Cookson) were diluted immediately before use and

applied acutely by bath superfusion. Recording pipettes were filled with (in mM) K-gluconate 125, KCl 13, HEPES 10, EGTA 10, and MgATP 2 (pH 7.2 with KOH) for all electrophysiological recordings. Data were collected using a Multiclamp 700A amplifier (2 kHz 8-pole Bessel filter), Digidata 1322 A/D converter, and sampled at 10 kHz using pCLAMP software (all from Axon Instruments, Union City, CA).

All recordings were obtained from neurons in the suprapyramidal dentate gyrus/hilus following $\geqslant$20 min of NMDAR antagonist washout. Recordings were conducted at room temperature (RT) to minimize the likelihood of electrographic seizures during antagonist washout (Bausch *et al*, 2006; Bausch and McNamara, 2000, 2004). Data for action potential and membrane properties were collected using current-clamp recording within 2 min of establishing whole-cell configuration. The resting membrane potential (RMP) was documented using Multiclamp software. Input resistance (R_{in}) was calculated from the slope of the linear portion of a current–voltage plot of the change in membrane voltage in response to a series of 450 ms 25-pA steps using pClamp software. The first current step eliciting an action potential was deemed the action potential threshold. The first action potential elicited at threshold was used to document action potential properties. Action potential rise and decay times were measured from 10% to 100% and from 100% to 10%, respectively; half-width was defined as the half-amplitude duration; fast afterhyperpolarization potential (fAHP) was measured from baseline just before action potential rise to hyperpolarized potential peak immediately following the action potential (Faber and Sah, 2002). Spontaneous firing was measured for 5–10 min in aCSF using somatic cell-attached recordings.

For voltage-clamp recordings of synaptic currents, the membrane potential was clamped at −70 mV, and recordings were excluded if series resistance was >15 MΩ or varied >15% or RMP was more positive than −50 mV for granule cells and −40 mV for interneurons. Spontaneous inhibitory postsynaptic currents (sIPSCs) were recorded in the presence of D-APV (50 μM) and CNQX (10 μM). The mIPSCs were recorded after subsequent addition of TTX (1 μM). All sIPSCs and mIPSCs were analyzed using MiniAnalysis software (Synaptosoft, Fort Lee, NJ). Detection threshold was 8 pA. Rise and decay times were measured from 10% to 100% and from 100% to 10%, respectively. Up to 80 events from each cell were selected at a fixed sampling interval to generate cumulative probability plots.

For paired recordings, presynaptic neurons were current-clamped to generate action potentials and postsynaptic neurons were voltage-clamped at −70 mV to record postsynaptic responses. An action potential was elicited in the presynaptic neuron using a 5 ms depolarizing current injection, which was minimally sufficient to evoke a single action potential. Failure rate was measured by delivering 50 depolarizing stimuli at 0.3 Hz to the presynaptic neuron and defined as the percentage of action potential-inducing stimuli that evoked no postsynaptic response. Paired-pulse ratio was measured by delivering 2 stimuli with a 100 ms interstimulus interval to the presynaptic neuron and defined as the amplitude of the second postsynaptic response normalized to the first.

Neurobiotin

Interneurons were filled with neurobiotin (0.4–0.5% (w/v) in the pipette solution; Vector, Burlingame, CA) during whole-cell recordings and visualized as described previously (Bausch *et al*, 2006). Briefly, immediately after recordings, cultures were fixed overnight with 4% paraformaldehyde in 0.1 M phosphate buffer (PB, pH 7.4), removed from the insert membrane, sunk in 30% sucrose in 0.1 M PB containing 0.15 M NaCl and 2.7 mM KCl (PBS, pH 7.4), and stored at −70 °C. Thawed cultures were treated with 10% methanol and 0.6% H_2O_2 in PBS, blocked with 2% bovine serum albumin (BSA) and 0.75% Triton X-100 in PBS and incubated overnight at 4 °C in ABC elite (Vector) diluted per kit instructions in PBS containing 2% BSA and 0.1% Triton X-100. Cultures were then treated with 0.05% 3,3′-diaminobenzidine (DAB, Sigma), 0.028% $CoCl_2$, 0.02% $NiSO_4 \cdot (NH_4)SO_4$, and 0.00075% H_2O_2 in PBS until staining was apparent. Cultures were mounted onto subbed glass slides, dehydrated, cleared, and coverslipped. Representative interneurons were photographed and/or manually reconstructed using Neurolucida software (MicroBrightField, Colchester, VT), a Zeiss (Thornwood, NY) Axioskop microscope equipped with 63× oil objective, MicroFire CCD camera (Optronics, Goleta, CA), and motorized stage and focus encoder (Ludl Electronic Products, Exton, PA) as described previously (Bausch *et al*, 2006). Regions were defined as: molecular layer, supragranular dentate gyrus regions; granule cell layer, tightly packed granule cell layer; hilus, region between granule cell layer blades excluding the CA3c pyramidal cell layer; and CA3c, pyramidal cell layers residing in the dentate gyrus. D/H border interneurons were classified based on axonal distribution and firing properties as shown in Figure 3 and described in Figure 3 legend.

Immunohistochemistry

Slice cultures were fixed with Formaldehyde/Zinc fixative (3.7% formaldehyde; Electron Microscopy Sciences, Fort Washington, PA) for 12 min and removed from the insert membrane. Free-floating slice cultures were processed for immunohistochemistry at RT unless stated otherwise. Slice cultures were pretreated sequentially with: 0.3% H_20_2 in 100% methanol; 10 mM Tris/1 mM EDTA (pH 9) for 20 min at 90 °C for antigen retrieval; 10% avidin followed by 10% biotin in PBS; and PBS containing 10% normal goat serum and 2% gelatin for 1 h at 37 °C. Slice cultures were then incubated in mouse monoclonal anti-Kv1.2 IgG2b (1 : 40; clone K14/16), Kv1.3 IgG1 (1 : 1000; clone L23/27), or Kv1.6 IgG3 (1 : 10; clone K19/36) (all from UC Davis/NINDS/NIMH NeuroMab Facility, Davis, CA) for 1 h at RT followed by ∼36 h at 4 °C. All antibodies were diluted in PBS containing 10% normal goat serum, 2% BSA, and 0.25% Triton X-100. Slice cultures were then incubated sequentially in biotinylated goat anti-mouse IgG (Vector) diluted 1 : 400 in diluent for 1 h and ABC Elite diluted in PBS containing 1% BSA and 0.1% Triton X-100 per kit instructions for 1 h at 37 °C. Immunoreactivity was visualized with 0.04% DAB and 0.0024% H_20_2 in TB. Slice cultures were mounted onto subbed glass slides, dehydrated, cleared, and coverslipped with Permount mounting media. Slice cultures were digitally photographed using a Zeiss Axioskop microscope, Optronics Microfire camera,

and Picture Frame software (Optronics). Immunoreactivity was quantified with MetaMorph software (Universal Imaging/Molecular Devices, Downingtown, PA) using a representative $50 \times 75\,\mu m$ area in the suprapyramidal dentate molecular layer and a $50 \times 75\,\mu m$ area in CA1 stratum lacunosum moleculare. Vehicle- and NMDAR antagonist-treated slice cultures were always processed in parallel to prevent nonspecific differences in intensity levels.

Statistics

Investigators were blinded to experimental groupings for all data analyses. Parametric data were represented as means ± SEM. Nonparametric data were represented as medians. Most statistical analyses were performed with Sigma Stat software (SPSS, Chicago, IL). Parametric data were tested for significance using an ANOVA with Holm–Sidak *post-hoc* comparison (multiple groups), *t*-test (two groups), or paired *t*-test (before and after acute drug application). Nonparametric data were tested using ANOVA on ranks (multiple groups) or Mann–Whitney rank sum test (two groups). Significance was defined as $p \leqslant 0.05$. Cumulative probability distributions were tested for significance using a two-tailed Kolmogorov–Smirnov test using MiniAnalysis software; significance was defined as $p \leqslant 0.025$.

RESULTS

The Frequency of Action Potential-Dependent sIPSCs But Not Action Potential-Independent mIPSCs onto Dentate Granule Cells Was Decreased Following Chronic Inhibition of NR2B-Containing NMDARs

To begin to examine changes in GABAergic neurotransmission following chronic NMDAR inhibition, we first measured sIPSCs in individual dentate granule cells in the presence of D-APV and CNQX to block excitatory transmission using whole-cell voltage-clamp recordings. We found a large shift in cumulative probability (Figure 1c) and a 70 ± 7% reduction in mean (Figure 1e) action potential-dependent sIPSC frequency following chronic inhibition of NR2B-containing NMDARs with Ro25,6981. This reduction was accompanied by a strong trend toward reduced near-synchronous sIPSCs (ie, ⩽10 ms interpeak interval; Schoppa and Westbrook, 2002; Figure 1a) following chronic Ro25,6981 (3.4 ± 0.8% of sIPSCs) compared with vehicle (5.9 ± 1.3%; $p = 0.056$, Mann–Whitney rank sum test). No large changes in sIPSC frequency were observed following chronic NMDAR inhibition with the NR2A-prefering antagonist, NVP-AAM077, or the non-subunit-selective NMDAR antagonist, D-APV (Figure 1c and e). Cumulative probabilities of sIPSC amplitude were modestly reduced (Figure 1d), but the average sIPSC amplitude was not significantly altered (Figure 1f) and changes in sIPSC kinetics were minimal (Supplementary Figure 1a). Action potential-independent mIPSC frequencies (Figure 2c and e) and amplitudes (Figure 2d and f) were only minimally altered following chronic NMDAR inhibition, although mIPSC rise time was reduced following chronic Ro25,6981 treatment (Supplementary Figure 1b). These data strongly suggest that the large reduction in sIPSC frequency following chronic Ro25,6981 was not mediated by alterations in PSC amplitude or changes in individual synapses as gauged by mIPSC frequency and amplitude.

The Frequency of Action Potential-Dependent sIPSCs But Not Action Potential-Independent mIPSCs onto Dentate/Hilar Border Interneurons was Decreased Following Chronic Inhibition of NR2B-Containing NMDARs

We next examined whether the effects of NMDAR antagonists on IPSCs were specific to dentate granule cells or also occurred in D/H border interneurons, which provide strong inhibition onto granule cells. Altered inhibition onto interneurons could affect presynaptic action potential-dependent GABA release by changing interneuron excitability. D/H border interneurons fell into five distinct categories based upon axonal distribution and firing pattern (see Figure 3 and its legend) as described previously (Buckmaster and Schwartzkroin, 1995a, b; Halasy and Somogyi, 1993; Han *et al*, 1993; Mott *et al*, 1997), except everywhere cells, which were described by Mott *et al* (1997) but named here. Briefly, axoaxonic cell axons displayed chandelier-like rows of boutons and projected predominantly to the granule cell and the CA3c pyramidal cell layers. Basket cell axons were restricted almost entirely to the granule cell layer. Both axoaxonic and basket cells were characterized by high-frequency, nonadapting firing. Hilar commissural-associational pathway-associated interneuron (HICAP cell) axonal collaterals were distributed predominantly in the outer granule cell layer and inner molecular layer. Hilar perforant pathway-related interneuron (HIPP cell) axonal collaterals were distributed predominantly in the outer molecular layer. Everywhere cell axons arborized radially throughout the dentate gyrus, hilus, and CA3 pyramidal cell layer. HICAP, HIPP, and everywhere cells were defined by adapting firing and spike broadening with diminished spike amplitude at suprathreshold current steps (see Figure 3 legend for a more thorough description of interneuron subtypes). As no significant differences in sIPSC or mIPSC frequency or amplitude were apparent between different D/H border interneuron populations, sIPSC and mIPSC data from all interneurons were pooled. Comparison of different treatment groups revealed a 66 ± 7% reduction in mean action potential-dependent sIPSC frequency in D/H border interneurons following chronic inhibition of NR2B-containing NMDAR with Ro25,6981, but no significant changes following chronic NMDAR inhibition with the NR2A-prefering antagonist, NVP-AAM077, or the non-subunit-selective NMDAR antagonist, D-APV (Figure 4a1). Mean sIPSC amplitude in D/H border interneurons was not significantly altered following chronic NMDAR inhibition with any antagonist, but a trend ($p = 0.110$, ANOVA with Holm–Sidak *post-hoc* comparison) toward decreased amplitude was observed following chronic inhibition of NR2B-containing NMDARs with Ro25,6981 (Figure 4a2). Average action potential-independent mIPSC frequency and amplitude in D/H border interneurons were not changed significantly following chronic NMDAR inhibition (Figure 4b). The similar effects of chronic NMDAR inhibition on IPSCs in interneurons and granule cells suggest that reduced sIPSC frequency in granule cells was not caused by increased inhibition onto interneurons and that plasticity

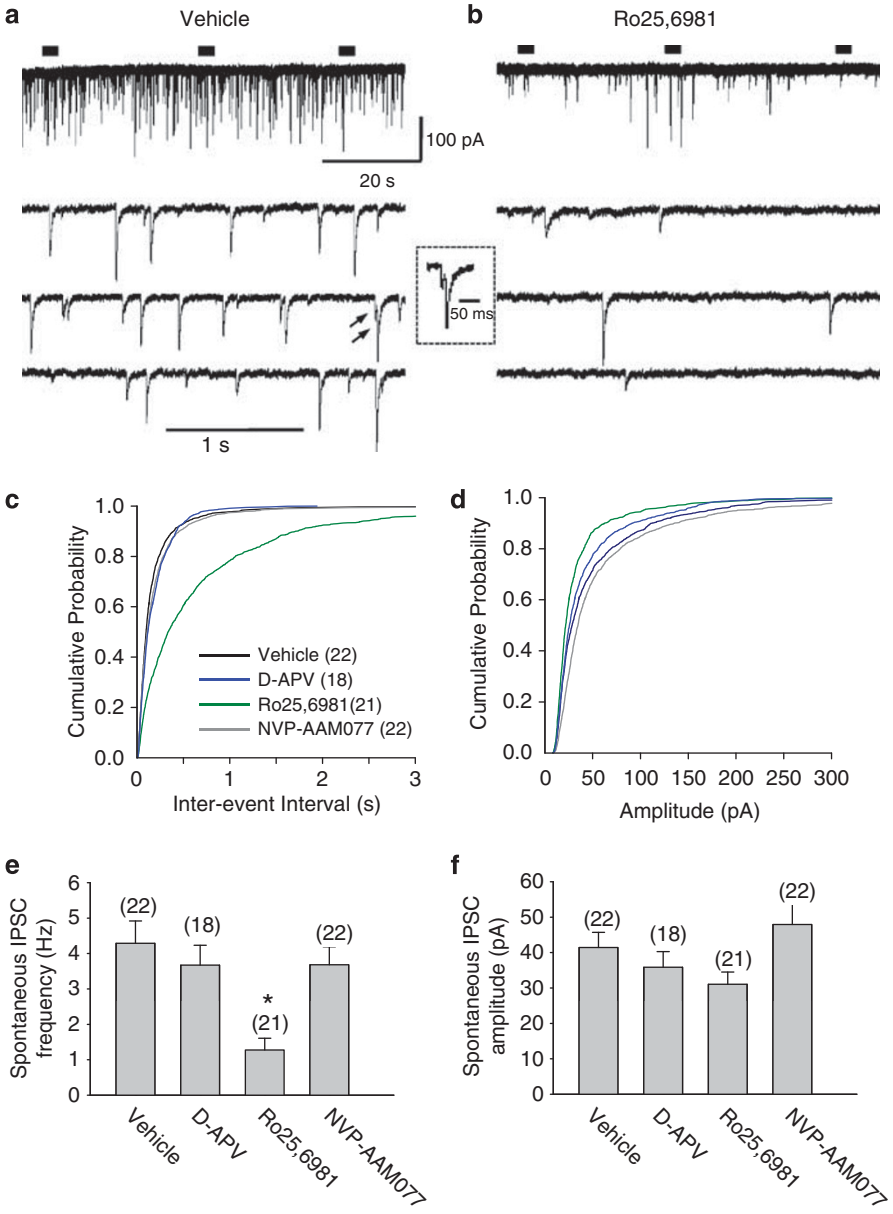

Figure 1 Spontaneous IPSC frequency was reduced in granule cells from hippocampal slice cultures treated chronically with Ro25,6981. Spontaneous IPSCs were recorded at a −70 mV holding potential in recording buffer containing D-APV (50 μM) and CNQX (10 μM). (a, b) Representative sIPSC recordings following chronic (a) vehicle or (b) Ro25,6981 in granule cells illustrate the large reductions in sIPSC frequency with only modest reductions in sIPSC amplitude. Arrows indicate near-synchronous sIPSCs, shown in an expanded timescale in the inset. (c, d) Cumulative probability plots reveal (c) slight but significant changes in sIPSC frequency following chronic NVP-AAM077 and D-APV, but dramatically reduced sIPSC frequency following chronic Ro25,6981. (d) They also show modestly reduced sIPSC amplitude following chronic treatment with all the NMDAR antagonists (difference in sIPSC frequency and amplitude between all treatment groups, $p<0.025$, Kolmogorov–Smirnov test). (e, f) Bar graphs reveal that sIPSC (e) frequency was dramatically reduced but (f) amplitude was not significantly altered in granule cells following chronic Ro25,6981 treatment. Scale bars in (a, middle) apply to (a) and (b). Legend in (c) applies to (c) and (d). The number of granule cells/slice cultures is indicated in parentheses. *Different than vehicle, D-APV, and NVP-AAM077; $p<0.05$, ANOVA with Holm–Sidak *post-hoc* comparison.

induced by chronic inhibition of NR2B-containing NMDARs in sIPSC frequency may occur in widespread interneuron subpopulations.

Intrinsic Active and Passive Membrane Properties Were Not Altered Following Chronic Inhibition of NR2B-Containing NMDARs

The lack of large changes in mIPSC frequency or amplitude (Figure 2) together with no change in GABAergic interneuron number or GABAergic synapses onto granule cells (Wang and Bausch, 2006) following chronic Ro25,6981 treatment suggest that altered synapse number cannot account for reduced sIPSC frequency. Altered excitatory transmission onto interneurons also cannot account for reduced sIPSC frequency because all IPSCs were recorded in the presence of D-APV and CNQX to block excitatory transmission. Therefore, the simplest and most likely explanation is a change in interneuron action potential and/or intrinsic membrane properties. Whole-cell

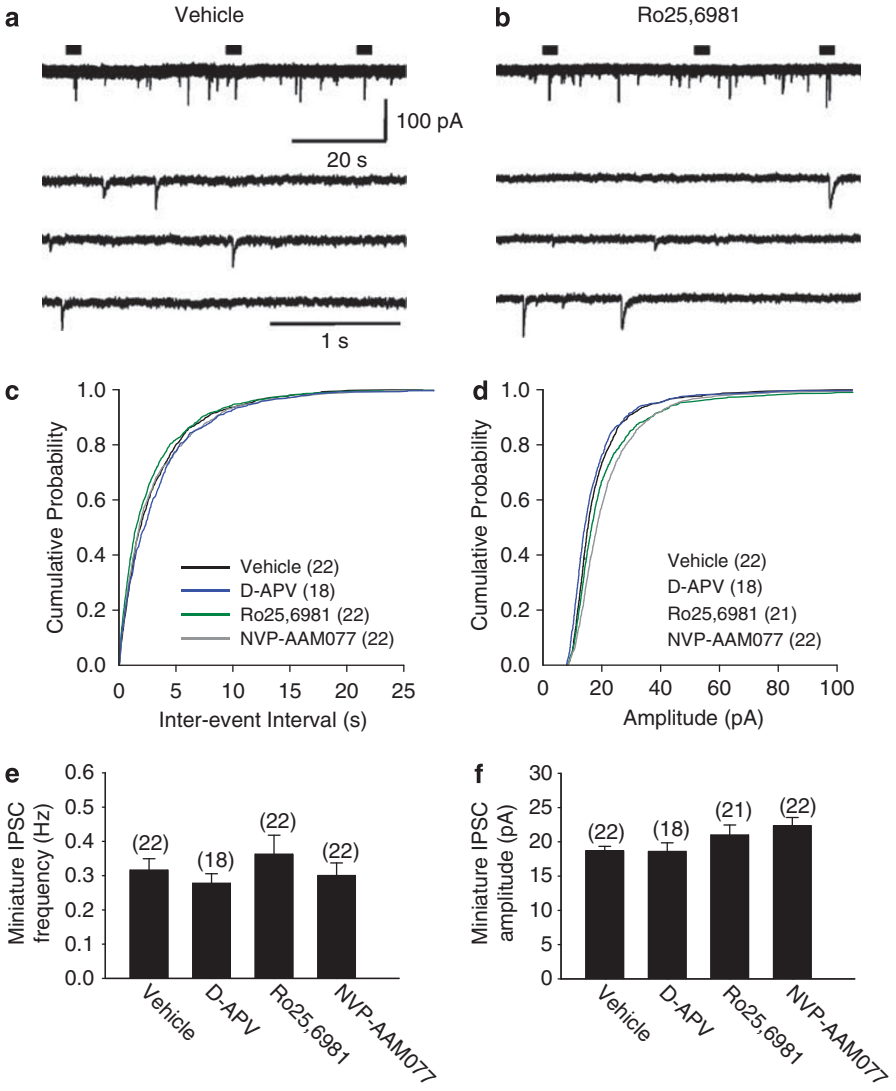

Figure 2 Miniature IPSC frequency and amplitude were minimally altered in granule cells from hippocampal slice cultures treated chronically with NMDAR antagonists. Miniature IPSCs were recorded at a −70 mV holding potential in recording buffer containing D-APV (50 μM), CNQX (10 μM), and TTX (1 μM). (a, b) Representative mIPSC recordings following chronic (a) vehicle or (b) Ro25,6981 in granule cells illustrate little change in mIPSC frequency or amplitude. (c, d) Cumulative probability plots reveal (c) minor changes in mIPSC frequency and (d) slight increases in mIPSC amplitude following chronic treatment with NVP-AAM077 or Ro25,6981 (difference in mIPSC frequency and amplitude between all treatment groups except vehicle *vs* D-APV, $p < 0.025$, Kolmogorov–Smirnov test). (e, f) Bar graphs reveal that mIPSC (e) frequency and (f) amplitude in granule cells were not significantly altered following chronic treatment with NMDAR antagonists. Scale bars in (a, middle) apply to (a) and (b). Legend in (c) applies to (c) and (d). The number of granule cells/slice cultures is indicated in parentheses.

current-clamp recordings were grouped by interneuron class because these membrane and action potential properties were different in distinct interneuron populations (Table 1). Comparing effects of chronic treatment with different NMDAR antagonists, we found a significantly more positive RMP and increased action potential half-width and rise and decay times in axoaxonic cells following chronic treatment with D-APV and NVP-AAM077, respectively (Table 1). However, no other significant effects of chronic NMDAR inhibition on input resistance, RMP, afterhyperpolarization, or action potential threshold, amplitude, half-width, rise, or decay were detected in D/H border interneurons (Table 1). Input–output curves of interneuron firing were grouped into high-frequency and adapting firing interneurons because the firing behavior was different across but not within these populations. The number of action potentials generated in response to current steps was not significantly altered in high-frequency firing interneurons following chronic treatment with NMDAR antagonists, but was increased in adapting firing interneurons following chronic treatment with D-APV or NVP-AAM077 compared with vehicle or Ro25,6981 (Figure 5). Somatic cell-attached recordings showed low spontaneous firing frequency in all interneuron populations and revealed no chronic Ro25,6981-mediated decreases in spontaneous interneuron firing rate ($n = 7$, vehicle; $n = 7$, Ro25,6981, data not shown). These data suggest that altered somatic action potential and membrane properties were

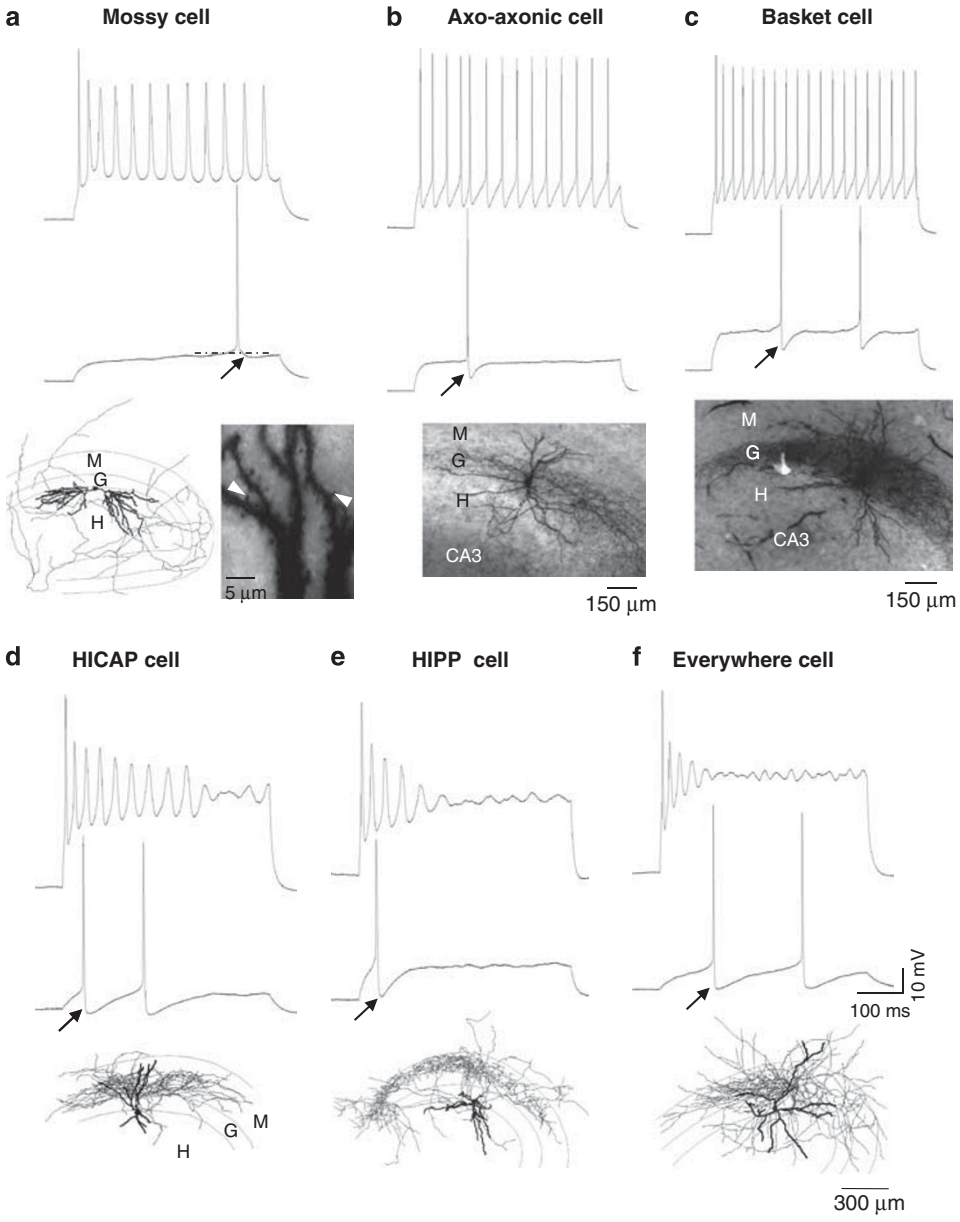

Figure 3 Firing patterns and axonal distributions were used to classify different types of interneurons. Interneurons were characterized as described previously (Buckmaster and Schwartzkroin, 1995a, b; Halasy and Somogyi, 1993; Han *et al*, 1993; Mott *et al*, 1997) except everywhere cells, which were described by Mott *et al* (1997) but named here. (a–e, top) Representative traces from the first current step to elicit strong adaptation and spike broadening in HICAP, HIPP, and everywhere cells, and a corresponding current step amplitude for mossy, axoaxonic, and basket cells. (a–e, middle) Representative traces from the first current step to elicit an action potential. (a–e, bottom) Representative morphology and axonal distributions of neurobiotin-filled neurons. (a) Mossy cells were characterized by high-frequency firing, a shallow AHP (dashed line, plateau potential), dendrites covered with dense 'thorny excrescences' (bottom right, white arrowheads), and axons distributed throughout the dentate gyrus and hilus. Recorded cells with these characteristics were excluded from further analyses. (b) Axoaxonic cells were characterized by high-frequency firing, action potentials with deep, short-duration AHP, as well as large somata, chandelier-like rows of boutons and axonal arborizations predominantly in the granule cell and the CA3c pyramidal cell layers. (c) Basket cells displayed high-frequency firing, action potentials with deep, short-duration AHP, and large somata and axons almost entirely restricted to the granule cell layer with net-like boutons surrounding granule cells. (d) Hilar commissural-associational pathway-associated interneurons (HICAP cells) were defined by adapting firing, deep, long-lasting AHP, and axonal collaterals distributed predominantly in the outer granule cell layer and the inner one-third of the molecular layer. Dendrites usually bifurcated bidirectionally into the molecular layer after crossing the granule cell layer and the hilus, and were either aspiny or sparsely spiny. (e) Hilar perforant pathway-related interneurons (HIPP cells) were characterized by adapting firing, deep intermediate-lasting AHP, and axonal collaterals distributed predominantly in the outer two-third of the molecular layer. Dendrites were often restricted to the hilus and covered with long thin spines. (f) Everywhere cells were characterized by adapting firing, deep long-duration AHP and axons that arborized radially throughout all regions of the dentate gyrus, hilus, and the CA3 pyramidal cell layer. Representative mossy, axoaxonic, basket, HICAP, HIPP, and everywhere cells were taken from Ro25,6981-, Ro25,6981-, vehicle-, D-APV-, memantine-, and NVP-AAM077-treated cultures, respectively. Arrows in (a–f, middle) indicate AHP. Scale bars in (f, middle) apply to all electrophysiological traces; scale bar in (f, bottom) applies to all digitally reconstructed neurons in (a, d–f). Thick black lines in all digitally reconstructed neurons denote dendrites, thin gray lines denote axons, and thin gray lines delineate regions. BC, basket cell; EC, everywhere cell; g, granule cell layer; h, hilus; HICAP cell, hilar commissural-associational pathway-associated interneuron; HIPP cell, hilar perforant pathway-associated interneuron; m, molecular layer.

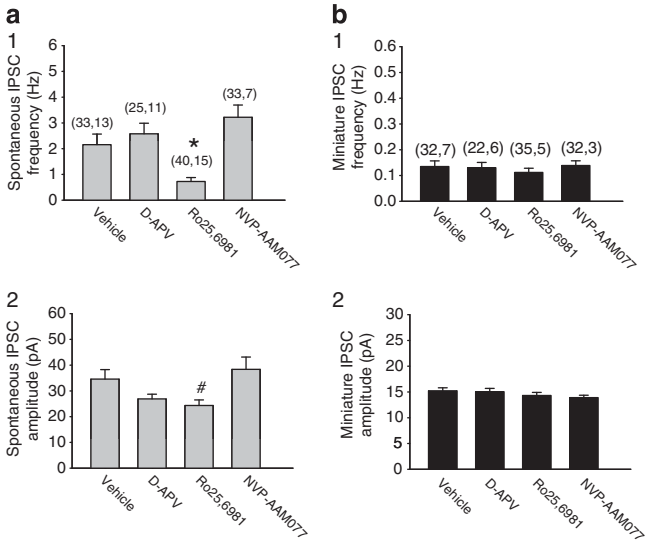

Figure 4 Spontaneous IPSC frequency was reduced in dentate/hilar border interneurons from hippocampal slice cultures treated chronically with Ro25,6981. Spontaneous IPSCs and mIPSCs were recorded as described in Figures 1 and 2, respectively. No significant differences between different D/H border interneuron populations were apparent, and data from all interneurons were compiled. Bar graphs reveal that compared with vehicle (a) sIPSC (a1) frequency was dramatically reduced but (a2) amplitude was not significantly altered in interneurons following chronic treatment with Ro25,6981. (b) Miniature IPSC (b1) frequency and (b2) amplitude in interneurons were not significantly altered following chronic treatment with NMDAR antagonists. The number of interneurons/slice cultures is indicated in parentheses as (adapting firing interneurons, high-frequency firing interneurons). *Different than vehicle, D-APV, and NVP-AAM077; #Different than NVP-AAM077; $p<0.05$, ANOVA with Holm–Sidak *post-hoc* comparison.

unlikely to account for the dramatically reduced sIPSC frequency after chronic inhibition of NR2B-containing NMDAR.

Action Potential-Dependent Release Probability Was Unaltered Following Chronic Inhibition of NR2B-Containing NMDARs

Fredj and Burrone (2009) recently demonstrated distinct vesicle pools for action potential-dependent and action potential-independent neurotransmitter release at CNS synapses. Reduced action potential-dependent release probability could decrease sIPSC frequency. Therefore, action potential-dependent release probability was documented using paired recordings between D/H border interneurons and dentate granule cells. All IPSCs evoked in interneuron–granule cell pairs (eIPSCs) should be monosynaptic because minimal inhibitory currents hyperpolarize rather than depolarize postsynaptic neurons, and eIPSCs in granule cells displayed a single, short latency distribution (1.89 ± 0.07 ms; range, 0.5–4.9 ms). Evoked IPSC failure data were grouped into high-frequency (basket and axoaxonic cells) and adapting (HIPP, HICAP, and everywhere cells) firing interneurons because the eIPSC failure rate was different across but not within these populations (Maccaferri *et al*, 2000; Xiang *et al*, 2002). Chronic treatment with NMDAR antagonists had no significant effect on eIPSC failure rate in either high-frequency (Figure 6b) or adapting firing (Figure 6c) interneurons. As failure rate measures a combination of release probability and axon conduction failure, we further investigated alterations in release probability using paired-pulse stimulation of presynaptic interneurons and recordings of subsequent paired-pulse IPSC ratios in granule cells. Paired stimuli with a 100 ms interstimulus interval were used to document release probability without the confound of high-frequency action potential-induced conduction failure (Debanne, 2004). Paired-pulse ratios were not significantly different in distinct populations of D/H border interneurons, and hence data from all interneuron–granule cell pairs were pooled. Chronic treatment with NMDAR antagonists did not significantly affect paired-pulse eIPSC ratios (Figure 6e), suggesting no change in action potential-dependent GABA release probability.

Finally, changes in presynaptic $GABA_B$ and group III metabotropic glutamate receptor (mGluR) function could alter action potential-dependent release probability and reduce sIPSC frequency (Niswender *et al*, 2008; Olpe *et al*, 1982). However, this possibility is unlikely because acute pharmacological blockade of $GABA_B$ receptors and group III mGluR with CGP55845 (3 μM) and CPPG (200 μM), respectively, had no impact on sIPSC frequency or amplitude in granule cells from either vehicle- or Ro25,6981-treated cultures (Figure 7). Taken together, these data suggest that alterations in action potential-dependent release probability could not account for reduced sIPSC frequency following chronic inhibition of NR2B-containing NMDARs.

Acute Blockade of Kv Channels with 4-AP or TEA Occluded the Effect of Chronic Inhibition of NR2B-Containing NMDARs on sIPSC Frequency

Acute pharmacological blockade or genetic deletion of voltage-gated potassium (Kv) channels can increase action potential-dependent GABA release (Cunningham and Jones, 2001; Goldberg *et al*, 2005; Southan and Robertson, 1998; Zhang *et al*, 1999) by modulating neuronal membrane potential and/or action potential threshold, duration, and frequency. Although we found no significant alterations in somatic membrane or action potential properties, changes in axonal properties could reduce sIPSC frequency by altering axonal excitability (Debanne, 2004; Dodson and Forsythe, 2004; Meir *et al*, 1999), which would not be detected using whole-cell or somatic cell-attached recordings. Therefore, we first tested whether two broad Kv channel blockers, 4-AP and TEA, applied acutely during recordings of sIPSCs, but after chronic NMDAR inhibition, could occlude the large reductions in sIPSC frequency observed following chronic inhibition of NR2B-containing NMDARs. Concentration-response experiments were conducted because blocker potency can provide clues as to the identity of altered Kv channels. Concentration-response analyses revealed that as little as 10 μM 4-AP or 20 mM TEA was sufficient to occlude the effects of chronic Ro25,6981 on sIPSC frequency in granule cells (Figure 8). Based on previously reported potencies for recombinant Kv channels (Judge and Bever, 2006; Mathie *et al*, 1998), no Kv channel subtype strictly fit our data. However, native endogenous Kv channels are unlikely to be homotetramers, but rather

Table 1 Membrane Properties in D/H Interneurons

Treatment	R_{IN} (MΩ)	RMP (mV)	Action potential					
			Threshold (mV)	Amplitude (mV)	Half-width (ms)	Rise time (ms)	Decay time (ms)	fAHP (mV)
Axoaxonic cell								
Vehicle	70 ± 4 (15)	−58.1 ± 0.9 (14)	−35.0 ± 0.5 (15)	69 ± 2 (15)	0.92 ± 0.04 (15)	0.36 ± 0.01 (15)	0.96 ± 0.05 (15)	−13.7 ± 0.6 (15)
D-APV	79 ± 4 (5)	−52.4 ± 0.9 (5)[a,b,c]	−32.7 ± 1.0 (5)	63 ± 3 (5)	0.97 ± 0.10 (5)	0.46 ± 0.04 (5)	0.92 ± 0.10 (5)	−13.9 ± 1.7 (5)
Ro25,6981	82 ± 7 (10)	−56.6 ± 0.4 (10)	−33.3 ± 0.9 (10)	64 ± 3 (10)	0.93 ± 0.07 (10)	0.41 ± 0.03 (10)	0.89 ± 0.09 (10)	−14.4 ± 0.6 (10)
NVP-AAM077	86 ± 9 (8)	−56.4 ± 0.9 (9)	−34.2 ± 1.1 (8)	65 ± 3 (8)	1.38 ± 0.14 (8)[a,b,d]	0.53 ± 0.03 (8)[a,b]	1.53 ± 0.23 (8)[a,b,d]	−13.5 ± 1.0 (8)
Basket cell								
Vehicle	58 ± 4 (7)	−56.5 ± 0.6 (7)	−33.3 ± 0.9 (7)	64 ± 2 (7)	1.03 ± 0.04 (7)	0.41 ± 0.01 (7)	1.05 ± 0.06 (7)	−15.1 ± 0.9 (7)
D-APV	77 ± 4 (10)	−56.0 ± 0.7 (10)	−31.4 ± 0.9 (10)	61 ± 2 (10)	1.00 ± 0.05 (10)	0.46 ± 0.03 (10)	0.97 ± 0.06 (10)	−16.4 ± 0.7 (10)
Ro25,6981	72 ± 6 (9)	−56.4 ± 0.4 (9)	−30.7 ± 1.0 (9)	58 ± 2 (9)	0.92 ± 0.07 (9)	0.44 ± 0.03 (9)	0.83 ± 0.07 (9)	−15.6 ± 0.6 (9)
NVP-AAM077	62 (1)	−58.7 (1)	−38.3 (1)	76 (1)	0.56 (1)	0.31 (1)	0.46 (1)	−10.1 (1)
HICAP cell								
Vehicle	211 ± 64 (3)	−53.5 ± 1.3 (3)	−33.7 ± 1.1 (3)	61 ± 7 (3)	2.9 ± 0.8 (3)	0.89 ± 0.35 (3)	3.08 ± 0.67 (3)	−9.3 ± 2.1 (3)
D-APV	190 ± 91 (3)	−51.7 ± 2.5 (3)	−33.8 ± 0.5 (3)	58 ± 3 (3)	2.17 ± 0.59 (3)	0.67 ± 0.19 (3)	2.40 ± 0.57 (3)	−11.2 ± 2.2 (3)
Ro25,6981	176 ± 47 (7)	−54.6 ± 1.3 (7)	−34.0 ± 0.7 (7)	64 ± 3 (7)	1.80 ± 0.18 (7)	0.70 ± 0.06 (7)	1.93 ± 0.25 (7)	−11.6 ± 1.3 (7)
NVP-AAM077	237 ± 29 (3)	−51.3 ± 0.5 (4)	−34.9 ± 0.9 (3)	73 ± 3 (3)	1.70 ± 0.24 (3)	0.58 ± 0.02 (3)	1.86 ± 0.20 (3)	−13.0 ± 1.39 (3)
HIPP cell								
Vehicle	166 ± 35 (6)	−54.5 ± 1.7 (8)	−34.6 ± 1.2 (6)	64 ± 2 (6)	1.66 ± 0.19 (6)	0.63 ± 0.08 (6)	1.63 ± 0.20 (6)	−13.6 ± 1.8 (6)
D-APV	234 ± 47 (6)	−50.9 ± 1.1 (7)	−33.6 ± 0.8 (6)	64 ± 3 (6)	1.99 ± 0.27 (6)	0.66 ± 0.06 (6)	2.18 ± 0.24 (6)	−11.2 ± 1.4 (6)
Ro25,6981	276 ± 47 (11)	−53.2 ± 1.2 (13)	−33.9 ± 1.0 (11)	61 ± 4 (11)	2.56 ± 0.29 (11)	0.87 ± 0.09 (11)	2.71 ± 0.30 (11)	−11.9 ± 1.1 (11)
NVP-AAM077	248 ± 42 (5)	−51.4 ± 1.3 (7)	−32.8 ± 1.7 (5)	63 ± 5 (5)	2.06 ± 0.21 (5)	0.81 ± 0.14 (5)	2.22 ± 0.38 (5)	−13.3 ± 2.4 (5)
Everywhere cell								
Vehicle	254 ± 22 (33)	−51.5 ± 0.6 (37)	−35.4 ± 0.4 (34)	65 ± 1 (34)	2.33 ± 0.12 (33)	0.78 ± 0.03 (33)	2.62 ± 0.14 (34)	−11.1 ± 0.5 (34)
D-APV	244 ± 26 (25)	−50.8 ± 0.6 (29)	−35.2 ± 0.4 (26)	65 ± 1 (26)	2.29 ± 0.17 (25)	0.72 ± 0.04 (25)	2.57 ± 0.18 (26)	−11.0 ± 0.7 (26)
Ro25,6981	266 ± 17 (28)	−52.2 ± 0.6 (31)	−34.6 ± 0.5 (28)	62 ± 2 (28)	2.47 ± 0.14 (28)	0.83 ± 0.05 (28)	2.64 ± 0.17 (28)	−11.1 ± 0.7 (28)
NVP-AAM077	295 ± 23 (33)	−53.1 ± 0.4 (35)	−35.2 ± 0.5 (33)	65 ± 2 (33)	2.26 ± 0.10 (33)	0.76 ± 0.03 (33)	2.49 ± 0.12 (33)	−11.6 ± 0.5 (33)

Abbreviations: fAHP, fast after hyperpolarization potential; HICAP cell, hilar commissural-associational pathway-associated cell; HIPP cell, hilar perforant pathway-related cell; R_{IN}, input resistance; RMP, resting membrane potential.
[a]Different than vehicle.
[b]Different than Ro25,6981.
[c]Different than NVP-AAM077.
[d]Different than D-APV.
Means ± SEM.
The number of granule cell/hippocampal slice cultures is indicated in parentheses.
$P < 0.05$, ANOVA with Holm–Sidak *post-hoc* comparison.

heterotetramer assemblies containing variable Kv1 subunits. Pharmacology, biophysical properties, expression, trafficking, and localization of Kv1 channels are influenced by coassembly of heteromeric Kv1 subunits, presence of β-subunits, composition of membrane lipids, glycosylation, phosphorylation, as well as the expression system, and the amount of mRNA injected into oocytes (Harvey, 1997; Mathie *et al*, 1998; Oliver *et al*, 2004; Robertson, 1997; Trimmer and Rhodes, 2004; reviews). That said, occlusion of chronic Ro25,6981-mediated effects by 10 μM 4-AP in our experiments suggested Kv3 involvement (Grissmer *et al*, 1994; Lien *et al*, 2002). Arguing against this possibility, Kv3 channels modulate action potential duration and are expressed predominantly in parvalbumin-containing axoaxonic and basket cells (Gan and Kaczmarek, 1998; Rudy and McBain, 2001), and we found no significant changes in action potential decay in axoaxonic or basket cells following chronic Ro25,6981 treatment. Moreover, 0.2 mM TEA, which selectively blocks Kv3 channels (Aiyar *et al*, 1994), did not significantly affect sIPSCs following chronic Ro25,6981 treatment. Occlusion of chronic Ro25,6981-mediated decreases in sIPSC frequency by 20 mM TEA implicated increased Kv1.1, Kv1.2, Kv1.3, and/or Kv2.1 channel function (Judge and Bever, 2006; Mathie *et al*,

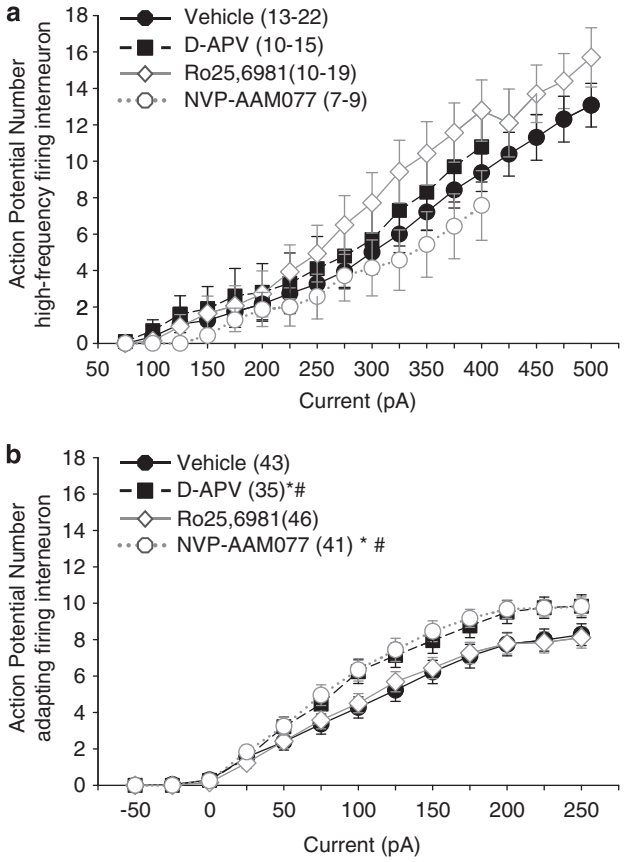

Figure 5 Action potential firing was increased in adapting firing interneurons from hippocampal slice cultures treated chronically with D-APV and NVP-AAM077. Whole-cell current-clamp recordings were conducted as described in the Materials and methods to determine the number of action potentials fired in response to a series of 450 ms 25 pA steps. Input–output curves were grouped into (a) high-frequency (basket and axoaxonic cells) and (b) adapting (HIPP, HICAP, and everywhere cells) firing interneurons because the firing behavior was different across but not within these populations. The number of action potentials generated by current steps above 250 pA was not quantified in adapting firing interneurons because spike number reached a plateau and the spikes were significantly wider in half-width and greatly diminished in amplitude (see Figure 3d–f), making the action potential difficult to precisely define. The number of action potentials generated in response to current steps (a) was not significantly altered in high-frequency firing interneurons following chronic treatment with NMDAR antagonists, but (b) was increased in adapting firing interneurons following chronic treatment with D-APV or NVP-AAM077 compared with vehicle or Ro25,6981. Note the difference in the *x*-axis scale in (a) and (b). The number of interneuron/slice cultures is indicated in parentheses. *Different than vehicle; #Different than Ro25,6981; $p<0.05$, two-way ANOVA with Holm–Sidak *post-hoc* comparison.

1998). Arguing against altered Kv2.1 channel function, Kv2.1 channels are expressed predominantly in somata and are critically involved in action potential and membrane property regulation (Misonou *et al*, 2005), but somatic action potential and membrane properties in interneurons were not significantly changed by chronic Ro25,6981 treatment. Therefore, we concentrated on potential alterations in Kv1 function because Kv1 channels are localized predominantly to axons and are implicated in regulation of presynaptic neurotransmitter release (Lai and Jan, 2006; Southan and Robertson, 1998; Zhang *et al*, 1999).

Enhanced Kv1 Channel Function Contributed to Reduced sIPSC Frequency Following Chronic Inhibition of NR2B-Containing NMDARs

To test the possibility that altered Kv1 channel function contributed to chronic Ro25,6981-mediated decreases in sIPSC frequency, we first acutely applied relatively broad Kv1 channel blockers. Acute Kv1.1, Kv1.2, and Kv1.6 blockade with α-dendrotoxin (200 nM; Grissmer *et al*, 1994; Lambe and Aghajanian, 2001; Figure 9a) or Kv1.1, Kv1.3, and Kv1.6 with agitoxin (30 nM; Garcia *et al*, 1994; Southan and Robertson, 1998) (not shown) dramatically increased sIPSC frequency in granule cells from Ro25,6981-treated cultures and, more importantly, occluded chronic Ro25,6981-induced decreases in sIPSC frequency. However, these toxins increased sIPSC frequency to maximal levels. Therefore, we next utilized more specific Kv blockers to minimize potential confounds of a ceiling effect and to more precisely define Kv1 channel subtype involvement. Acute blockade of Kv1.3-containing channels with margatoxin (10 nM; Akhtar *et al*, 2002; Southan and Robertson, 2000) modestly increased sIPSC frequency and also completely occluded chronic Ro25,6981-mediated decreases in sIPSC frequency (Figure 9b). Acute blockade of Kv1.1-containing Kv1 channels with dendrotoxin-K (100 nM; Vicente *et al*, 2006) modestly increased sIPSC frequency and amplitude, but did not occlude chronic Ro25,6981-mediated decreases in sIPSC frequency (Figure 9c). Another Kv channel, Kv7, is expressed in hippocampal and dentate gyrus interneurons, can colocalize with Kv1 channels in axonal initial segments, juxtaparanodal regions, and synaptic terminals, and can modulate interspike interval and GABA release (Cooper *et al*, 2001; Devaux *et al*, 2004; Lai and Jan, 2006; Lawrence *et al*, 2006; Martire *et al*, 2004; Trimmer and Rhodes, 2004). Therefore, a specific Kv7 channel blocker was used as a control to show specificity of Ro25,6981-mediated effects on Kv1 channel function. Acute pharmacological blockade of Kv7 with XE 991 (10 μM) did not significantly affect sIPSC frequency or amplitude in granule cells and did not occlude chronic Ro25,6981-mediated effects on sIPSC frequency (Figure 9d, Ro25,6981/vehicle = approximately 50%, $p=0.12$, *t*-test). The negative outcome with XE 991 is consistent with the findings of Martire *et al* (2004), who showed that 10 μM XE 991 blocked retigabine-mediated increases in high K^+-induced neurotransmitter release from synaptosomes but had no effect alone. Taken together, our findings imply that upregulated Kv1 channel function reduced sIPSC frequency following chronic inhibition of NR2B-containing NMDARs with Ro25,6981 and that these channels contain Kv1.3, Kv1.6, and possibly Kv1.2. As Kvα1.3 and Kvα1.6 can form a tetramer with Kvα1.2/1.4 and Kvβ2 (Shamotienko *et al*, 1997), the Kv1 channels underlying chronic Ro25,6981-mediated effects on sIPSC frequency are likely to be heteromeric complexes.

Kv1 Channel Expression Was Increased in the Dentate Molecular Layer Following Chronic Inhibition of NR2B-Containing NMDARs

Finally, we used immunohistochemistry to examine Kv1.2, Kv1.3, and Kv1.6 protein levels in the dentate gyrus. Kv1.2 and Kv1.3 were significantly increased in the dentate

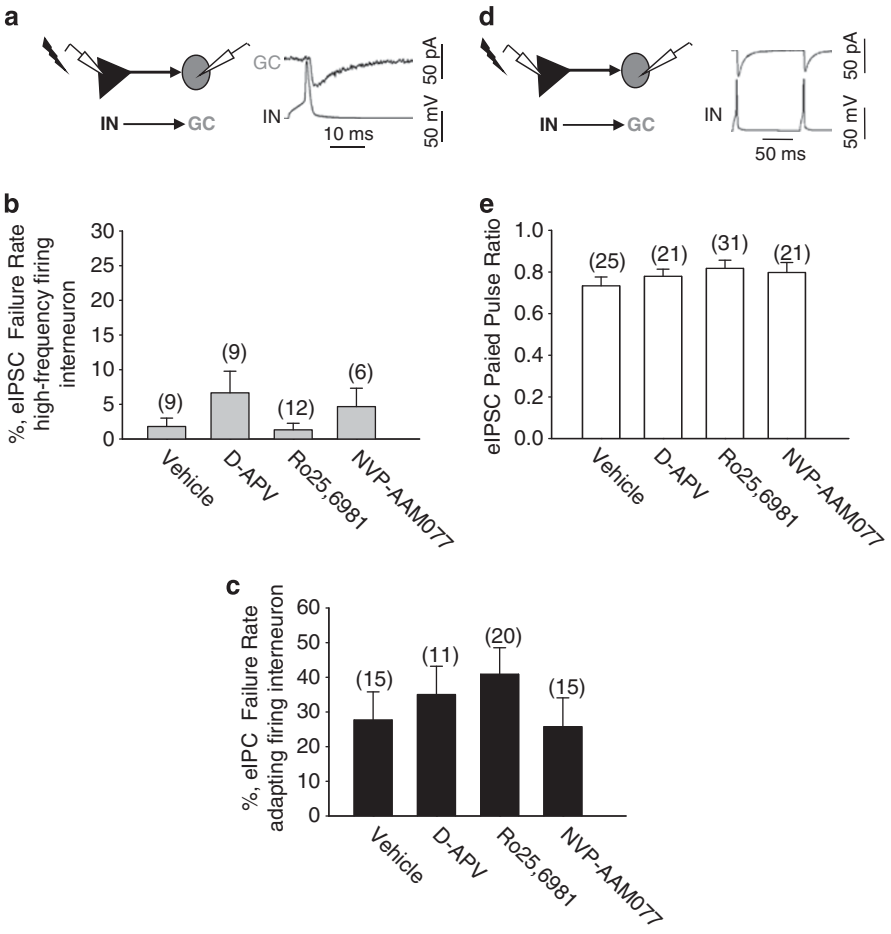

Figure 6 Evoked IPSC (eIPSC) failure rate and paired-pulse ratio were similar in granule cells from cultures treated with vehicle and NMDAR antagonists. Paired whole-cell recordings between single dentate granule cells and D/H border interneurons were conducted as described in the Materials and methods to document eIPSC failure rate and release probability. (a, left) A schematic of a paired recording between a single interneuron and granule cell. (a, right) A representative trace of an evoked action potential in the presynaptic interneuron and the subsequent eIPSC in a postsynaptic granule cell from a vehicle-treated culture. Failure data were grouped into high-frequency (basket and axoaxonic cells) and adapting (HIPP, HICAP, and everywhere cells) firing interneurons because the failure rate was different across but not within these populations. Bar graphs reveal no significant changes in eIPSC failure rate in granule cells following repeated action potential generation in either (b) high-frequency firing interneurons (axoaxonic and basket cells) or (c) adapting firing interneurons (HICAP, HIPP, and everywhere cells) following chronic NMDAR inhibition. Note the difference in the *y*-axis scale in (b) and (c). (d, left) A schematic of a paired recording from an interneuron to a granule cell and (d, right) a representative trace of a pair of evoked action potentials in a presynaptic interneuron and subsequent a pair of evoked IPSCs in a postsynaptic granule cell from a vehicle-treated culture. (e) Bar graph reveals no significant difference in eIPSC paired-pulse ratio between individual interneurons and granule cells in different treatment groups. Data were grouped for all D/H interneurons because there was no significant difference between distinct types of interneurons (data not shown). The number of slice cultures is indicated in parentheses. GC, granule cell; IN, interneuron.

molecular layer following chronic Ro25,6981 compared with vehicle. Kv1.2 and Kv 1.6 were significantly higher following chronic Ro25,6981 compared with vehicle when immunoreactivity in the molecular layer was normalized to that in CA1 stratum lacunosum moleculare in each slice culture (Figure 10). Taken together with electrophysiological results, our findings suggest that increased Kv1.2, Kv1.3, and Kv1.6 expression mediated the large reductions in sIPSC frequency following chronic inhibition of NR2B-containing NMDARs.

DISCUSSION

Large reductions in sIPSC frequency were observed in both dentate granule cells and interneurons following chronic inhibition of NR2B-containing NMDARs with Ro25,6981. However, mean sIPSC amplitude, mIPSC frequency, and mIPSC amplitude were not significantly altered, suggesting diminished action potential-dependent GABA release. Chronic treatment with NVP-AAM077 or D-APV had minimal effects on these measures. Reduced sIPSC frequency following chronic Ro25,6981 was not due to downregulated $GABA_AR$ because mIPSC amplitude was only modestly altered. Decreased excitatory or increased inhibitory drive to interneurons did not reduce sIPSC frequency because fast excitatory transmission was blocked and sIPSC frequency in interneurons was reduced. Reduced sIPSC frequency did not arise from altered somatic interneuron membrane/action potential properties because these properties were largely unchanged. Altered action potential-dependent release probability and mGluR/$GABA_B$

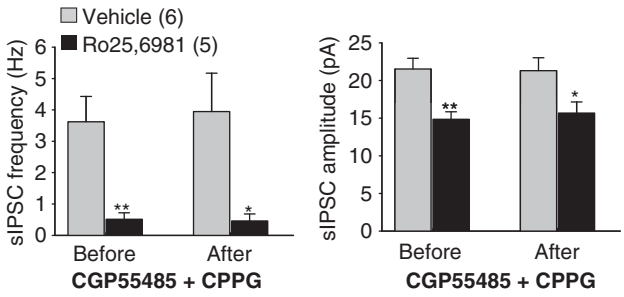

Figure 7 The frequency and amplitude of sIPSCs in granule cells were unchanged after blockade of $GABA_B$ receptors and group III metabotropic glutamate receptors (mGluR). Spontaneous IPSCs were recorded as described in the Materials and methods and Figure 1. Bar graphs revealed that acute blockade of $GABA_BR$ with CGP55845 (3 μM) and group III mGluR with CPPG (200 μM) did not affect sIPSC (left) frequency or (right) amplitude in granule cells from cultures treated with vehicle or Ro25,6981. Legend in (left) applies to (left) and (right). The number of granule cells/slice cultures is indicated in parentheses; $*p<0.05$; $**p<0.01$, different than vehicle, *t*-test.

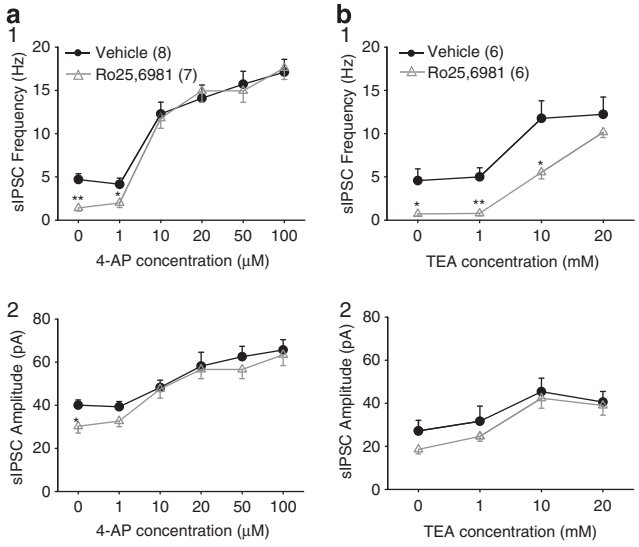

Figure 8 Two broad-acting voltage-gated potassium channel antagonists abolished the difference in sIPSCs onto granule cells in vehicle- and Ro25,6981-treated cultures. Spontaneous IPSCs were recorded as described in the Materials and methods and Figure 1. Concentration-response curves showed that as little as 10 μM 4-aminopyridine (4-AP) abolished the differences in sIPSC (a1) frequency and (a2) amplitude. Concentration-response curves showed that 20 mM tetraethylammonium (TEA) abolished the differences in sIPSC (b1) frequency and (b2) amplitude between vehicle- and Ro25,6981-treated cultures. Legend in (a1) applies to (a1–2), and in (b1) applies to (b1–2). The number of slice cultures is indicated in parentheses; $*p<0.05$; $**p<0.01$, different than vehicle, *t*-test.

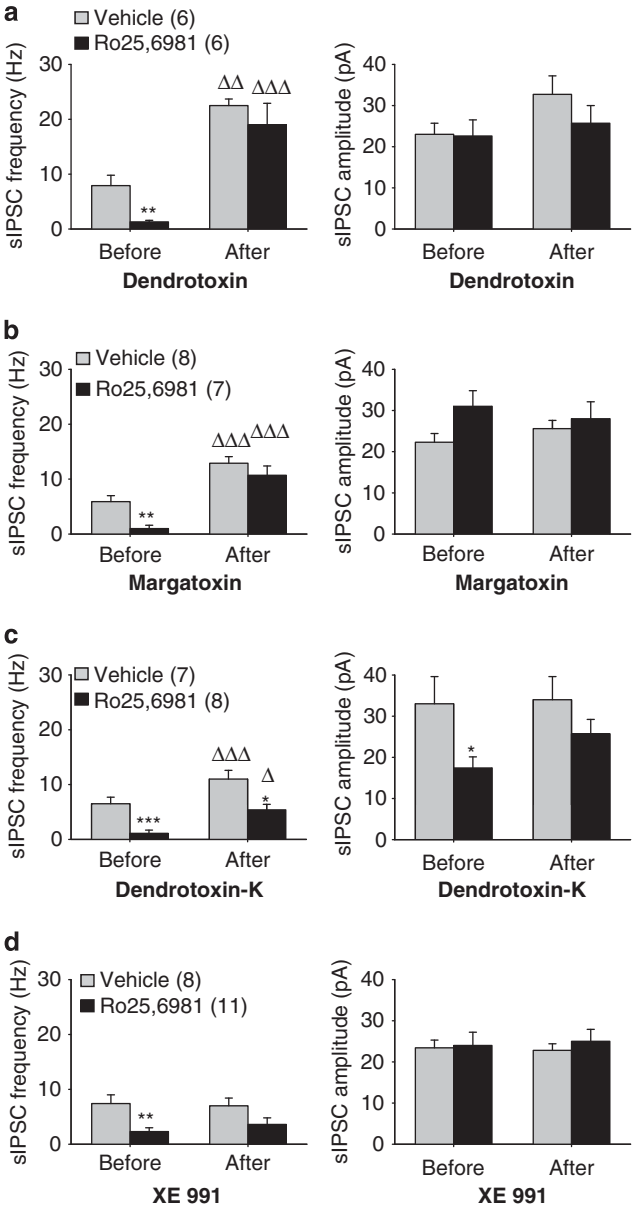

Figure 9 Acute blockade of Kv1 but not Kv7 channels occluded reductions in sIPSC frequency following chronic inhibition of NR2B-containing NMDARs. Recordings of sIPSCs in granule cells were conducted as described in the Materials and methods and Figure 1. Acute application of Kv1 channel blockers (a) dendrotoxin (200 nM) or (b) margatoxin (10 nM) occluded the difference between chronic vehicle and Ro25,6981 treatment in (a, b left) sIPSC frequency, but had no significant effect on (a, b right) sIPSC amplitude. Acute application of (c) dendrotoxin-K (100 nM) increased (c, left) sIPSC frequency in granule cells from both vehicle- and Ro25,6981-treated cultures, but did not occlude the difference between chronic vehicle and Ro25,6981 treatment and had little effect on (c, right) sIPSC amplitude. Acute blockade of Kv7 channels with (d) XE 991 (10 μM) had no effect on (d, left) sIPSC frequency or (d, right) amplitude in granule cells from either vehicle- and Ro25,6981-treated cultures. Legend in (a–d, left) applies to (a–d, left and right). 'Before' denotes measurements taken before acute application of blockers, and 'after' denotes measurements taken after acute application of blockers in the same cells. The number of granule cells is indicated in parentheses; $*p<0.05$; $**p<0.01$, $***p<0.001$ different than vehicle, *t*-test. $^{\Delta}p<0.05$; $^{\Delta\Delta}p<0.01$; $^{\Delta\Delta\Delta}p<0.001$ different than before in same chronic treatment group, paired *t*-test.

receptor modulation of GABA release cannot account for reduced sIPSC frequency because paired granule cell/interneuron recordings revealed no significant change in eIPSC failure rate or paired-pulse ratio, and mGluR and $GABA_B$ receptor inhibitors did not affect sIPSC frequency. However, chronic Ro25,6981-mediated reductions in sIPSC frequency were occluded by dendrotoxin, margatoxin, agitoxin but not dendrotoxin-K or XE 991, and immunohistochemistry revealed increased Kv1.2, Kv1.3, and Kv1.6

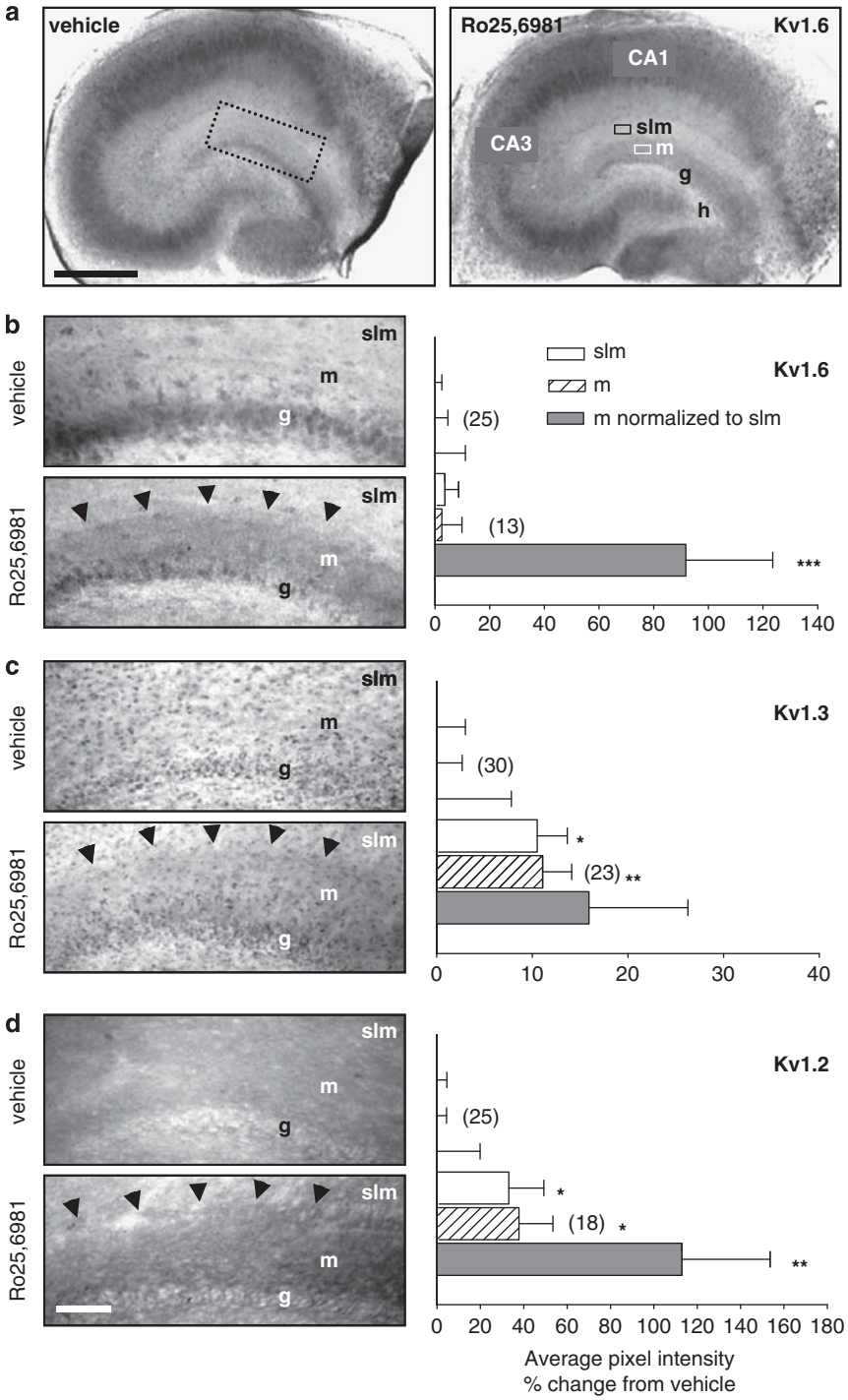

Figure 10 Kv1 channel expression was significantly increased in the dentate molecular layer in hippocampal slice cultures treated chronically with Ro25,6981. Hippocampal slice cultures were stained immunohistochemically for Kv1.2, Kv1.3, and Kv1.6 and analyzed as described in the Materials and methods. (a) Representative low-power images of Kv1.6 immunoreactivity in organotypic hippocampal slice cultures treated with (left) vehicle or (right) Ro25,6981. Dashed box (left) illustrates the approximate location of higher power images in (b–d). Black and white boxes (right) show the approximate locations for CA1 stratum lacunosum moleculare and dentate molecular layer quantification, respectively. (b–d) Representative higher-power images (left) and bar graphs of compiled quantification (right) of (b) Kv1.6, (c) Kv1.3, and (d) Kv1.2 immunoreactivity show increased expression (arrowheads) in the dentate molecular layer. The number of slice cultures is indicated in parentheses. Labels in (b–d, left) apply to micrographs (b–d, left) and bar graphs (b–d, right). Legend in (b, right) applies to (b–d, right) and represents the order of data presentation for both vehicle and Ro25,6981. Scale bar (a, left, 500 μm) applies to both panels in (a); (d, bottom, 100 μm) to all left panels in (b–d). g, granule cell layer; h, hilus; m, molecular layer; slm, stratum lacunosum moleculare. *$p<0.05$; **$p\leqslant0.01$; ***$p<0.005$, different than vehicle, Mann–Whitney rank sum test.

in the dentate molecular layer. Our findings suggest that increased Kv1 channel expression contributed to diminished action potential-dependent GABA release following chronic inhibition of NR2B-containing NMDARs and that these channels may be heteromeric complexes containing Kv1.2, Kv1.3, and Kv1.6. Our conclusions are consistent

with the predominant NR2B (Telfeian *et al*, 2003) and Kv1.6 expression in hippocampal interneurons and Kv1.2, 1.6, and β1 in dentate interneurons (Rhodes *et al*, 1997), as well as presynaptic Kv1.3 modulation of hippocampal GABA release (Ohno-Shosaku *et al*, 1996). To our knowledge, this is the first report showing large reductions in action potential-dependent GABA release and the involvement of increased Kv1 channel expression/function following chronic inhibition of NR2B-containing NMDARs.

Dichotomy Between Inhibition of NR2B-Containing NMDARs with Ro25,6981 and D-APV on sIPSC Frequency

At first pass the lack of similar effects of Ro25,6981 and D-APV on sIPSCs is somewhat surprising, given that both compounds inhibit NR2B-containing NMDARs. However, there is a stark difference between complete global blockade of NMDAR function with the competitive antagonist D-APV and partial inhibition of NR2B-containing NMDARs with the allosteric modulator Ro25,6981. Complete NMDAR blockade can be detrimental to neurons (Hardingham and Bading, 2003) and causes cognitive and psychotomimetic dysfunction. In contrast, partial inhibition of NR2B-containing NMDARs elicits few adverse effects clinically (Kemp and McKernan, 2002) and still maintains some level of physiological NMDAR function required for normal brain function. These differences place the neural circuits in very dissimilar states. Additionally, as described in the Introduction, NR2A- and NR2B-containing NMDARs are thought to play opposing roles in a variety of physiological processes. Conceptually, if basal activity is similar and NR2B is inhibited, NR2A effects would predominate. If basal activity is similar and both NR2A and NR2B are blocked, one would expect no change.

Potential Localization of Increased Kv1 Channel Expression/Function Responsible for Decreased sIPSC Frequency Following Chronic Inhibition of NR2B-Containing NMDARs

Potassium channels regulate neuronal excitability, axonal action potential propagation, and neurotransmitter release. Accordingly, Kv1 channels are localized predominantly to axons, but also reside in somata, dendrites (Arnold, 2007; Lai and Jan, 2006; Trimmer and Rhodes, 2004), and glia (Hallows and Tempel, 1998; Schlichter *et al*, 1996; Smart *et al*, 1997). Astrocytes modulate inhibitory neurotransmission (Kang *et al*, 1998; Yamazaki *et al*, 2005) and express Kv1.3, Kv1.6 (Lee *et al*, 2009; Smart *et al*, 1997), and NR2B-containing NMDARs (Conti *et al*, 1996). However, dendrotoxin is specific for neuronal Kv1 channels (Grissmer *et al*, 1994; Lambe and Aghajanian, 2001), suggesting that neuronal Kv1 upregulation contributed to reduced sIPSC frequency. Altered somatodendritic Kv1 channel function in interneurons was unlikely to reduce sIPSC frequency because mIPSC amplitude and somatic action potential/membrane properties were minimally affected. Thus, Kv1 channels responsible for reduced sIPSC frequency following chronic Ro25,6981 treatment likely reside in interneuron axons and/or synaptic terminals.

Axonal potassium channels control synaptic efficacy by influencing action potential invasion into nerve terminals (Lambe and Aghajanian, 2001) and reside in axonal initial segments (AISs), branch points, axonal swellings, juxtaparanodal regions, synaptic terminals, and preterminal axonal 'necks' (Cooper *et al*, 1998; Geiger and Jonas, 2000; Inda *et al*, 2006; Rhodes *et al*, 1997; Sheng *et al*, 1993; Van Wart *et al*, 2007; Zhang *et al*, 1999). Kv1 in the AIS dampens near-threshold excitability in fast-spiking interneurons (Goldberg *et al*, 2008). Therefore, upregulated AIS Kv1 channel function could lead to reduced sIPSC frequency. Arguing against this possibility, AIS is responsible for action potential initiation and we found no change in firing properties. Moreover, decreased sIPSC amplitude combined with increased mIPSC amplitude suggest that less neurotransmitter is released for a given action potential. Kv1 channels in branch points and axonal swellings influence conduction fidelity (Grossman *et al*, 1979; Krnjevic and Miledi, 1959), and Kv1 channels in synaptic terminals and preterminal necks modulate spike duration, terminal excitability, neurotransmitter release probability, and subsequent PSC amplitude (Geiger and Jonas, 2000). However, we detected no significant changes in IPSC failures or paired-pulse ratio, arguing against this possibility. Finally, Kv1.1 deletion at septate-like junctions increases cross-excitation of closely apposed axons (Chiu *et al*, 1999). By analogy, increased Kv1 function at septate-like junctions may decrease cross-activation between closely apposed axons, which would decrease coincident GABA release and thereby decrease sIPSC frequency without altering conduction failures or release probability in paired recordings between individual interneurons and granule cells. In partial support of this notion, reductions in near-synchronous sIPSCs and sIPSC amplitude were observed following chronic Ro25,6981 treatment. However, the reduction in sIPSC amplitude was modest and a low percentage of sIPSCs was near-synchronous, suggesting that decreased cross-activation between closely apposed axons alone is unlikely to fully explain the large reductions in sIPSC frequency. Further experimentation is clearly required to better define the localization(s) of increased Kv1 channel expression/function responsible for decreased sIPSC frequency following chronic inhibition of NR2B-containing NMDARs.

Potential Mechanisms Underlying Increased Kv1 Channel Function Following Chronic Inhibition of NR2B-Containing NMDARs

Previous studies showed that NMDAR activation alters Kv4.2 somatodendritic membrane surface expression and voltage-dependent channel inactivation (Kim *et al*, 2007; Lei *et al*, 2008) and changes Kv2.1 phosphorylation, somatic surface expression, lateral diffusion, and voltage-dependent channel activation (Misonou *et al*, 2004; Yao *et al*, 2009). Increased local intracellular calcium elicited directly by NMDAR activation and indirectly via membrane depolarization and subsequent voltage-gated Ca^{2+} channel activation are thought to underlie functional Kv channel modulation. Close spatial relationships between transient local NMDAR-mediated Ca^{2+} influx (Mainen *et al*, 1999; Sabatini *et al*, 2002) and Kv channels (Engelman

and MacDermott, 2004; Seifert and Steinhauser, 2001; Smart *et al*, 1997; Trimmer and Rhodes, 2004) are thought to underlie NMDAR modulation of somatodendritic Kv channels. However, in our study chronic inhibition of NR2B-containing NMDARs most likely altered axonal Kv1 channel function, raising the question of how chronic NMDAR inhibition modulated axonal Kv channels. Fiszman *et al* (2005) as well as Christie and Jahr (2008) reported that somatodendritic NMDAR currents are transmitted to cerebellar basket cell terminals via axonal electrotonic current propagation. These findings suggest that a close spatial NMDAR/Kv1 relationship is not necessary for NMDAR-mediated Kv1 channel regulation and support NMDAR modulation of axonal Kv1. Additionally, a variety of neuronal subtypes express presynaptic NR2B-containing NMDARs (Berretta and Jones, 1996; Brasier and Feldman, 2008; Sjostrom *et al*, 2003; Yang *et al*, 2006), including cerebellar interneurons (Christie and Jahr, 2008; Duguid and Smart, 2004; Fiszman *et al*, 2005; Glitsch and Marty, 1999; Huang and Bordey, 2004), which reside primarily in extrasynaptic axons (Gracy and Pickel, 1995; Gracy *et al*, 1997). Although similar findings have yet to be reported in hippocampal/dentate gyrus interneurons, these data provide possible scenarios by which NMDAR activation and by analogy blockade of dendritic and/or axonal NR2B-containing NMDARs could modulate axonal Kv channel function.

High NR2B expression in hippocampal interneurons (Telfeian *et al*, 2003) and unique biophysical properties of NR2B-containing NMDARs may account for the specific effects of chronic NR2B-containing NMDAR inhibition on Kv channel function. NR2B conveys higher Ca^{2+} permeability than NR2A and preferentially forms complexes with downstream Ca^{2+}-binding proteins like CaMKII (Leonard *et al*, 1999; Strack *et al*, 2000) and RasGRF1 (Krapivinsky *et al*, 2003). As elevated NMDAR-mediated Ca^{2+} influx reduces Kv channel membrane surface localization (Lei *et al*, 2008), chronic NR2B-containing NMDAR inhibition may increase Kv channel surface expression via diminished Ca^{2+} entry. NMDAR activation also increases Kv1 phosphorylation (Tao *et al*, 2005), which modulates channel conductance, open probability, and voltage sensitivity (Kwak *et al*, 1999a, b; Peretz *et al*, 1996; Vogalis *et al*, 1995), suggesting that altered phosphorylation, in addition to increased expression, may also increase Kv1 channel function (Tao *et al*, 2005).

Potential Role of Altered GABA Transmission and Kv1 Channel Function in Seizure Expression, Depression, and Other Neurological Disorders

Together with our previous results (Dong and Bausch, 2005; Wang and Bausch, 2006), we showed that reduced action potential-dependent GABA release onto dentate granule cells and interneurons is associated with upregulated Kv1 function and reduced seizure expression. In parallel, increased GABA release with unaltered glutamatergic transmission in cerebral cortex (van Brederode *et al*, 2001) was associated with spontaneous seizures in Kv1.1-null mice (Brew *et al*, 2007; Rho *et al*, 1999; Smart *et al*, 1998). Although the Kv1 channels underlying altered GABAergic inhibition are potentially different, both findings are at odds with data showing seizure control following therapeutic enhancement of GABAergic transmission and seizurogenic properties of $GABA_AR$ blockade (Burt, 1962; Paul *et al*, 1979). Additionally, although the mechanisms by which NMDAR antagonists reduce major depressive symptoms remain unclear, our findings of reduced action potential-dependent GABA release are at odds with the popular, but controversial, GABA-deficit hypothesis of major depression (Croarkin *et al*, 2010; Hasler, 2010; Luscher *et al*, 2010). These discrepancies suggest that: (1) either the described changes in GABAergic transmission do not influence seizure expression or major depressive symptoms, (2) or a simple imbalance between excitatory and inhibitory transmission does not underlie seizure genesis or major depression. Recent evidence suggests a bidirectional relationship between epilepsy and depression (ie, patients and animal models with one disorder are predisposed to the other), suggesting a potential common mechanism (Kanner, 2011).

In adult brain, GABAergic transmission elicits hyperpolarization via Cl^- influx and shunting inhibition via increased $GABA_A$ receptor-mediated membrane permeability (Mann and Paulsen, 2007). As the Cl^- reversal potential is close to the RMP in mature dentate granule cells (Scharfman, 1994; Staley and Mody, 1992; Williamson *et al*, 1995) and cortical pyramidal cells (Gulledge and Stuart, 2003), shunting inhibition predominates. Shunting inhibition primarily synchronizes neuronal firing rather than balancing excitation in the dentate gyrus (Vida *et al*, 2006). Therefore, diminished action potential-dependent GABAergic transmission elicited by chronic inhibition of NR2B-containing NMDARs may reduce synchronization of neuronal firing and subsequent seizure expression and/or depression. However, although synchronous neuronal firing is a hallmark of seizures, the role of neuronal synchrony in depression is unclear. Alternatively, reduced $GABA_B$ receptor activation can be antidepressant (Bowery, 2006; Ghose *et al*, 2010) and diminished action potential-dependent GABA release may reduce $GABA_B$ as well as $GABA_A$ activation. These two separate yet converging mechanisms could explain the bidirectional relationship between epilepsy and depression and the therapeutic efficacy of NR2B-selective NMDAR antagonists in both disorders. In summary, the precise mechanisms by which NR2B antagonists and/or reduced action potential-dependent GABA release exert therapeutic benefit in seizure expression, major depression, pain, and Parkinson's disease may depend upon GABA receptor subtypes, GABAergic interneuron synchrony, and/or NR2B-containing NMDAR localization relative to pathophysiological circuits.

ACKNOWLEDGEMENTS

We thank Dr Yves Auberson for his kind gift of NVP-AAM077, Dr Ed Cooper for helpful discussions, and Dr Zygmunt Galdzicki for critical reading of an earlier version of the manuscript. Work was supported by the Congressionally Directed Medical Research Programs award W81XWH-04-1-0065/PR030035 and National Institute of Neurological Disorders and Stroke grant NS045964. The monoclonal antibodies against Kv1.2, 1.3, and 1.6 were developed and obtained from the UC Davis/NINDS/NIMH NeuroMab Facility, supported by the NIH grant

U24NS050606 and maintained by the Department of Pharmacology, School of Medicine, University of California, Davis, CA. All treatment of animals complied with National Institutes of Health, Department of Defense and institutional guidelines.

DISCLOSURE

The authors declare that except for income received from their primary employers, no financial support or compensation has been received from any individual or corporate entity for research or professional service and there are no personal financial holdings that could be perceived as constituting a potential conflict of interest. The opinions or assertions contained herein are the private ones of the authors and are not to be construed as official or reflecting the views of the Department of Defense or the Uniformed Services University.

REFERENCES

Aiyar J, Nguyen AN, Chandy KG, Grissmer S (1994). The P-region and S6 of Kv3.1 contribute to the formation of the ion conduction pathway. *Biophys J* **67**: 2261–2264.

Akhtar S, Shamotienko O, Papakosta M, Ali F, Dolly JO (2002). Characteristics of brain Kv1 channels tailored to mimic native counterparts by tandem linkage of alpha subunits: implications for K+ channelopathies. *J Biol Chem* **277**: 16376–16382.

Arnold DB (2007). Polarized targeting of ion channels in neurons. *Pflugers Arch* **453**: 763–769.

Auberson YP, Allgeier H, Bischoff S, Lingenhoehl K, Moretti R, Schmutz M (2002). 5-Phosphonomethylquinoxalinediones as competitive NMDA receptor antagonists with a preference for the human 1A/2A, rather than 1A/2B receptor composition. *Bioorg Med Chem Lett* **12**: 1099–1102.

Barria A, Malinow R (2002). Subunit-specific NMDA receptor trafficking to synapses. *Neuron* **35**: 345–353.

Barria A, Malinow R (2005). NMDA receptor subunit composition controls synaptic plasticity by regulating binding to CaMKII. *Neuron* **48**: 289–301.

Bausch SB, He S, Petrova Y, Wang XM, McNamara JO (2006). Plasticity of both excitatory and inhibitory synapses is associated with seizures induced by removal of chronic blockade of activity in cultured hippocampus. *J Neurophysiol* **96**: 2151–2167.

Bausch SB, McNamara JO (2000). Synaptic connections from multiple subfields contribute to granule cell hyperexcitability in hippocampal slice cultures. *J Neurophysiol* **84**: 2918–2932.

Bausch SB, McNamara JO (2004). Contributions of mossy fiber and CA1 pyramidal cell sprouting to dentate granule cell hyperexcitability in kainic acid-treated hippocampal slice cultures. *J Neurophysiol* **92**: 3582–3595.

Bear MF, Kleinschmidt A, Gu QA, Singer W (1990). Disruption of experience-dependent synaptic modifications in striate cortex by infusion of an NMDA receptor antagonist. *J Neurosci* **10**: 909–925.

Berberich S, Punnakkal P, Jensen V, Pawlak V, Seeburg PH, Hvalby O *et al* (2005). Lack of NMDA receptor subtype selectivity for hippocampal long-term potentiation. *J Neurosci* **25**: 6907–6910.

Berretta N, Jones RS (1996). Tonic facilitation of glutamate release by presynaptic N-methyl-D-aspartate autoreceptors in the entorhinal cortex. *Neuroscience* **75**: 339–344.

Bowery NG (2006). GABAB receptor: a site of therapeutic benefit. *Curr Opin Pharmacol* **6**: 37–43.

Brasier DJ, Feldman DE (2008). Synapse-specific expression of functional presynaptic NMDA receptors in rat somatosensory cortex. *J Neurosci* **28**: 2199–2211.

Brew HM, Gittelman JX, Silverstein RS, Hanks TD, Demas VP, Robinson LC *et al* (2007). Seizures and reduced life span in mice lacking the potassium channel subunit Kv1.2, but hypoexcitability and enlarged Kv1 currents in auditory neurons. *J Neurophysiol* **98**: 1501–1525.

Buckmaster PS, Schwartzkroin PA (1995a). Interneurons and inhibition in the dentate gyrus of the rat in vivo. *J Neurosci* **15** (1 Pt 2): 774–789.

Buckmaster PS, Schwartzkroin PA (1995b). Physiological and morphological heterogeneity of dentate gyrus-hilus interneurons in the gerbil hippocampus in vivo. *Eur J Neurosci* **7**: 1393–1402.

Burt GS (1962). Strain differences in picrotoxin seizure threshold. *Nature* **193**: 301–302.

Chenard BL, Bordner J, Butler TW, Chambers LK, Collins MA, De Costa DL *et al* (1995). (1S,2S)-1-(4-hydroxyphenyl)-2-(4-hydroxy-4 phenylpiperidino)-1-propanol: a potent new neuroprotectant which blocks *N*-methyl-*D*-aspartate responses. *J Med Chem* **38**: 3138–3145.

Chiu SY, Zhou L, Zhang CL, Messing A (1999). Analysis of potassium channel functions in mammalian axons by gene knockouts. *J Neurocytol* **28**: 349–364.

Christie JM, Jahr CE (2008). Dendritic NMDA receptors activate axonal calcium channels. *Neuron* **60**: 298–307.

Church J, Fletcher EJ, Baxter K, MacDonald JF (1994). Blockade by ifenprodil of high voltage-activated Ca^{2+} channels in rat and mouse cultured hippocampal pyramidal neurones: comparison with *N*-methyl-*D*-aspartate receptor antagonist actions. *Br J Pharmacol* **113**: 499–507.

Cline HT, Debski EA, Constantine-Paton M (1987). N-methyl-D-aspartate receptor antagonist desegregates eye-specific stripes. *Proc Natl Acad Sci USA* **84**: 4342–4345.

Conti F, DeBiasi S, Minelli A, Melone M (1996). Expression of NR1 and NR2A/B subunits of the NMDA receptor in cortical astrocytes. *Glia* **17**: 254–258.

Cooper EC, Harrington E, Jan YN, Jan LY (2001). M channel KCNQ2 subunits are localized to key sites for control of neuronal network oscillations and synchronization in mouse brain. *J Neurosci* **21**: 9529–9540.

Cooper EC, Milroy A, Jan YN, Jan LY, Lowenstein DH (1998). Presynaptic localization of Kv1.4-containing A-type potassium channels near excitatory synapses in the hippocampus. *J Neurosci* **18**: 965–974.

Croarkin PE, Levinson AJ, Daskalakis ZJ (2010). Evidence for GABAergic inhibitory deficits in major depressive disorder. *Neurosci Biobehav Rev* **35**: 818–825.

Cunningham MO, Jones RS (2001). Dendrotoxin sensitive potassium channels modulate GABA but not glutamate release in the rat entorhinal cortex in vitro. *Neuroscience* **107**: 395–404.

Debanne D (2004). Information processing in the axon. *Nat Rev Neurosci* **5**: 304–316.

Devaux JJ, Kleopa KA, Cooper EC, Scherer SS (2004). KCNQ2 is a nodal K+ channel. *J Neurosci* **24**: 1236–1244.

Dingledine R, Borges K, Bowie D, Traynelis SF (1999). The glutamate receptor ion channels. *Pharmacol Rev* **51**: 7–61.

Dodson PD, Forsythe ID (2004). Presynaptic K+ channels: electrifying regulators of synaptic terminal excitability. *Trends Neurosci* **27**: 210–217.

Dong Y, Bausch SB (2005). Subunit selectivity contributes to differential effects of distinct classes of NMDAR antagonists on seizures in vitro. *Epilepsia* **46**(Suppl 8): 1.

Drejer J, Honore T, Schousboe A (1987). Excitatory amino acid-induced release of 3H-GABA from cultured mouse cerebral cortex interneurons. *J Neurosci* **7**: 2910–2916.

Duguid IC, Smart TG (2004). Retrograde activation of presynaptic NMDA receptors enhances GABA release at cerebellar interneuron-Purkinje cell synapses. *Nat Neurosci* **7**: 525–533.

Engelman HS, MacDermott AB (2004). Presynaptic ionotropic receptors and control of transmitter release. *Nat Rev Neurosci* **5**: 135–145.

Faber ES, Sah P (2002). Physiological role of calcium-activated potassium currents in the rat lateral amygdala. *J Neurosci* **22**: 1618–1628.

Feng B, Tse HW, Skifter DA, Morley R, Jane DE, Monaghan DT (2004). Structure-activity analysis of a novel NR2C/NR2D-preferring NMDA receptor antagonist: 1-(phenanthrene-2-carbonyl) piperazine-2,3-dicarboxylic acid. *Br J Pharmacol* **141**: 508–516.

Fischer G, Mutel V, Trube G, Malherbe P, Kew JN, Mohacsi E *et al* (1997). Ro 25-6981, a highly potent and selective blocker of N-methyl-D-aspartate receptors containing the NR2B subunit. Characterization in vitro. *J Pharmacol Exp Ther* **283**: 1285–1292.

Fiszman ML, Barberis A, Lu C, Fu Z, Erdelyi F, Szabo G *et al* (2005). NMDA receptors increase the size of GABAergic terminals and enhance GABA release. *J Neurosci* **25**: 2024–2031.

Flint AC, Maisch US, Weishaupt JH, Kriegstein AR, Monyer H (1997). NR2A subunit expression shortens NMDA receptor synaptic currents in developing neocortex. *J Neurosci* **17**: 2469–2476.

Fredj NB, Burrone J (2009). A resting pool of vesicles is responsible for spontaneous vesicle fusion at the synapse. *Nat Neurosci* **12**: 751–758.

Gan L, Kaczmarek LK (1998). When, where, and how much? Expression of the Kv3.1 potassium channel in high-frequency firing neurons. *J Neurobiol* **37**: 69–79.

Garcia ML, Garcia-Calvo M, Hidalgo P, Lee A, MacKinnon R (1994). Purification and characterization of three inhibitors of voltage-dependent K+ channels from Leiurus quinquestriatus var. hebraeus venom. *Biochemistry* **33**: 6834–6839.

Geiger JR, Jonas P (2000). Dynamic control of presynaptic Ca(2+) inflow by fast-inactivating K(+) channels in hippocampal mossy fiber boutons. *Neuron* **28**: 927–939.

Ghose S, Winter MK, McCarson KE, Tamminga CA, Enna SJ (2010). The GABAB receptor as a target for antidepressant drug action. *Br J Pharmacol* **162**: 1–17.

Glitsch M, Marty A (1999). Presynaptic effects of NMDA in cerebellar Purkinje cells and interneurons. *J Neurosci* **19**: 511–519.

Goldberg EM, Clark BD, Zagha E, Nahmani M, Erisir A, Rudy B (2008). K+ channels at the axon initial segment dampen near-threshold excitability of neocortical fast-spiking GABAergic interneurons. *Neuron* **58**: 387–400.

Goldberg EM, Watanabe S, Chang SY, Joho RH, Huang ZJ, Leonard CS *et al* (2005). Specific functions of synaptically localized potassium channels in synaptic transmission at the neocortical GABAergic fast-spiking cell synapse. *J Neurosci* **25**: 5230–5235.

Gracy KN, Pickel VM (1995). Comparative ultrastructural localization of the NMDAR1 glutamate receptor in the rat basolateral amygdala and bed nucleus of the stria terminalis. *J Comp Neurol* **362**: 71–85.

Gracy KN, Svingos AL, Pickel VM (1997). Dual ultrastructural localization of mu-opioid receptors and NMDA-type glutamate receptors in the shell of the rat nucleus accumbens. *J Neurosci* **17**: 4839–4848.

Grissmer S, Nguyen AN, Aiyar J, Hanson DC, Mather RJ, Gutman GA *et al* (1994). Pharmacological characterization of five cloned voltage-gated K+ channels, types Kv1.1, 1.2, 1.3, 1.5, and 3.1, stably expressed in mammalian cell lines. *Mol Pharmacol* **45**: 1227–1234.

Grossman Y, Parnas I, Spira ME (1979). Differential conduction block in branches of a bifurcating axon. *J Physiol* **295**: 283–305.

Gulledge AT, Stuart GJ (2003). Excitatory actions of GABA in the cortex. *Neuron* **37**: 299–309.

Halasy K, Somogyi P (1993). Subdivisions in the multiple GABAergic innervation of granule cells in the dentate gyrus of the rat hippocampus. *Eur J Neurosci* **5**: 411–429.

Hallows JL, Tempel BL (1998). Expression of Kv1.1, a Shaker-like potassium channel, is temporally regulated in embryonic neurons and glia. *J Neurosci* **18**: 5682–5691.

Han ZS, Buhl EH, Lorinczi Z, Somogyi P (1993). A high degree of spatial selectivity in the axonal and dendritic domains of physiologically identified local-circuit neurons in the dentate gyrus of the rat hippocampus. *Eur J Neurosci* **5**: 395–410.

Hardingham GE, Bading H (2003). The Yin and Yang of NMDA receptor signalling. *Trends Neurosci* **26**: 81–89.

Hardingham GE, Fukunaga Y, Bading H (2002). Extrasynaptic NMDARs oppose synaptic NMDARs by triggering CREB shut-off and cell death pathways. *Nat Neurosci* **5**: 405–414.

Harvey AL (1997). Recent studies on dendrotoxins and potassium ion channels. *Gen Pharmacol* **28**: 7–12.

Hasler G (2010). Pathophysiology of depression: do we have any solid evidence of interest to clinicians? *World Psychiatry* **9**: 155–161.

Huang H, Bordey A (2004). Glial glutamate transporters limit spillover activation of presynaptic NMDA receptors and influence synaptic inhibition of Purkinje neurons. *J Neurosci* **24**: 5659–5669.

Ikonomidou C, Bosch F, Miksa M, Bittigau P, Vockler J, Dikranian K *et al* (1999). Blockade of NMDA receptors and apoptotic neurodegeneration in the developing brain. *Science* **283**: 70–74.

Inda MC, DeFelipe J, Munoz A (2006). Voltage-gated ion channels in the axon initial segment of human cortical pyramidal cells and their relationship with chandelier cells. *Proc Natl Acad Sci USA* **103**: 2920–2925.

Judge SI, Bever Jr CT (2006). Potassium channel blockers in multiple sclerosis: neuronal Kv channels and effects of symptomatic treatment. *Pharmacol Ther* **111**: 224–259.

Kang J, Jiang L, Goldman SA, Nedergaard M (1998). Astrocyte-mediated potentiation of inhibitory synaptic transmission. *Nat Neurosci* **1**: 683–692.

Kanner AM (2011). Depression and epilepsy: a bidirectional relation? *Epilepsia* **52**(Suppl 1): 21–27.

Kemp JA, McKernan RM (2002). NMDA receptor pathways as drug targets. *Nat Neurosci* **5**(Suppl): 1039–1042.

Kim J, Jung SC, Clemens AM, Petralia RS, Hoffman DA (2007). Regulation of dendritic excitability by activity-dependent trafficking of the A-type K+ channel subunit Kv4.2 in hippocampal neurons. *Neuron* **54**: 933–947.

Krapivinsky G, Krapivinsky L, Manasian Y, Ivanov A, Tyzio R, Pellegrino C *et al* (2003). The NMDA receptor is coupled to the ERK pathway by a direct interaction between NR2B and RasGRF1. *Neuron* **40**: 775–784.

Krnjevic K, Miledi R (1959). Presynaptic failure of neuromuscular propagation in rats. *J Physiol* **149**: 1–22.

Kwak YG, Hu N, Wei J, George Jr AL, Grobaski TD, Tamkun MM *et al* (1999a). Protein kinase A phosphorylation alters Kvbeta1.3 subunit-mediated inactivation of the Kv1.5 potassium channel. *J Biol Chem* **274**: 13928–13932.

Kwak YG, Navarro-Polanco RA, Grobaski T, Gallagher DJ, Tamkun MM (1999b). Phosphorylation is required for alteration of kv1.5 K(+) channel function by the Kvbeta1.3 subunit. *J Biol Chem* **274**: 25355–25361.

Lai HC, Jan LY (2006). The distribution and targeting of neuronal voltage-gated ion channels. *Nat Rev Neurosci* **7**: 548–562.

Lambe EK, Aghajanian GK (2001). The role of Kv1.2-containing potassium channels in serotonin-induced glutamate release from thalamocortical terminals in rat frontal cortex. *J Neurosci* **21**: 9955–9963.

Lavezzari G, McCallum J, Dewey CM, Roche KW (2004). Subunit-specific regulation of NMDA receptor endocytosis. *J Neurosci* **24**: 6383–6391.

Lawrence JJ, Saraga F, Churchill JF, Statland JM, Travis KE, Skinner FK *et al* (2006). Somatodendritic Kv7/KCNQ/M channels control interspike interval in hippocampal interneurons. *J Neurosci* **26**: 12325–12338.

Lee SM, Kim JE, Sohn JH, Choi HC, Lee JS, Kim SH *et al* (2009). Down-regulation of delayed rectifier K+ channels in the hippocampus of seizure sensitive gerbils. *Brain Res Bull* **80**: 433–442.

Lei Z, Deng P, Xu ZC (2008). Regulation of Kv4.2 channels by glutamate in cultured hippocampal neurons. *J Neurochem* **106**: 182–192.

Leonard AS, Lim IA, Hemsworth DE, Horne MC, Hell JW (1999). Calcium/calmodulin-dependent protein kinase II is associated with the N-methyl-D-aspartate receptor. *Proc Natl Acad Sci USA* **96**: 3239–3244.

Lien CC, Martina M, Schultz JH, Ehmke H, Jonas P (2002). Gating, modulation and subunit composition of voltage-gated K(+) channels in dendritic inhibitory interneurones of rat hippocampus. *J Physiol* **538**(Pt 2): 405–419.

Lin SY, Constantine-Paton M (1998). Suppression of sprouting: an early function of NMDA receptors in the absence of AMPA/kainate receptor activity. *J Neurosci* **18**: 3725–3737.

Liu L, Wong TP, Pozza MF, Lingenhoehl K, Wang Y, Sheng M *et al* (2004). Role of NMDA receptor subtypes in governing the direction of hippocampal synaptic plasticity. *Science* **304**: 1021–1024.

Lu YM, Mansuy IM, Kandel ER, Roder J (2000). Calcineurin-mediated LTD of GABAergic inhibition underlies the increased excitability of CA1 neurons associated with LTP. *Neuron* **26**: 197–205.

Luscher B, Shen Q, Sahir N (2010). The GABAergic deficit hypothesis of major depressive disorder. *Mol Psychiatry* **16**: 383–406.

Maccaferri G, Roberts JD, Szucs P, Cottingham CA, Somogyi P (2000). Cell surface domain specific postsynaptic currents evoked by identified GABAergic neurones in rat hippocampus in vitro. *J Physiol* **524**(Pt 1): 91–116.

Mainen ZF, Malinow R, Svoboda K (1999). Synaptic calcium transients in single spines indicate that NMDA receptors are not saturated. *Nature* **399**: 151–155.

Mann EO, Paulsen O (2007). Role of GABAergic inhibition in hippocampal network oscillations. *Trends Neurosci* **30**: 343–349.

Marsden KC, Beattie JB, Friedenthal J, Carroll RC (2007). NMDA receptor activation potentiates inhibitory transmission through GABA receptor-associated protein-dependent exocytosis of GABA(A) receptors. *J Neurosci* **27**: 14326–14337.

Martire M, Castaldo P, D'Amico M, Preziosi P, Annunziato L, Taglialatela M (2004). M channels containing KCNQ2 subunits modulate norepinephrine, aspartate, and GABA release from hippocampal nerve terminals. *J Neurosci* **24**: 592–597.

Massey PV, Johnson BE, Moult PR, Auberson YP, Brown MW, Molnar E *et al* (2004). Differential roles of NR2A and NR2B-containing NMDA receptors in cortical long-term potentiation and long-term depression. *J Neurosci* **24**: 7821–7828.

Mathie A, Wooltorton JR, Watkins CS (1998). Voltage-activated potassium channels in mammalian neurons and their block by novel pharmacological agents. *Gen Pharmacol* **30**: 13–24.

Matthews DB, Kralic JE, Devaud LL, Fritschy JM, Marrow AL (2000). Chronic blockade of N-methyl-D-aspartate receptors alters gamma-aminobutyric acid type A receptor peptide expression and function in the rat. *J Neurochem* **74**: 1522–1528.

McCool BA, Lovinger DM (1995). Ifenprodil inhibition of the 5-hydroxytryptamine$_3$ receptor. *Neuropharmacology* **34**: 621–629.

McKinney RA, Luthi A, Bandtlow CE, Gahwiler BH, Thompson SM (1999). Selective glutamate receptor antagonists can induce or prevent axonal sprouting in rat hippocampal slice cultures. *Proc Natl Acad Sci USA* **96**: 11631–11636.

Meir A, Ginsburg S, Butkevich A, Kachalsky SG, Kaiserman I, Ahdut R *et al* (1999). Ion channels in presynaptic nerve terminals and control of transmitter release. *Physiol Rev* **79**: 1019–1088.

Misonou H, Mohapatra DP, Park EW, Leung V, Zhen D, Misonou K *et al* (2004). Regulation of ion channel localization and phosphorylation by neuronal activity. *Nat Neurosci* **7**: 711–718.

Misonou H, Mohapatra DP, Trimmer JS (2005). Kv2.1: a voltage-gated k+ channel critical to dynamic control of neuronal excitability. *Neurotoxicology* **26**: 743–752.

Mony L, Kew JN, Gunthorpe MJ, Paoletti P (2009). Allosteric modulators of NR2B-containing NMDA receptors: molecular mechanisms and therapeutic potential. *Br J Pharmacol* **157**: 1301–1317.

Monyer H, Burnashev N, Laurie DJ, Sakmann B, Seeburg PH (1994). Developmental and regional expression in the rat brain and functional properties of four NMDA receptors. *Neuron* **12**: 529–540.

Mori H, Mishina M (1995). Structure and function of the NMDA receptor channel. *Neuropharmacology* **34**: 1219–1237.

Morishita W, Lu W, Smith GB, Nicoll RA, Bear MF, Malenka RC (2007). Activation of NR2B-containing NMDA receptors is not required for NMDA receptor-dependent long-term depression. *Neuropharmacology* **52**: 71–76.

Moriyoshi K, Masu M, Ishii T, Shigemoto R, Mizuno N, Nakanishi S (1991). Molecular cloning and characterization of the rat NMDA receptor. *Nature* **354**: 31–37.

Mott DD, Turner DA, Okazaki MM, Lewis DV (1997). Interneurons of the dentate-hilus border of the rat dentate gyrus: morphological and electrophysiological heterogeneity. *J Neurosci* **17**: 3990–4005.

Neyton J, Paoletti P (2006). Relating NMDA receptor function to receptor subunit composition: limitations of the pharmacological approach. *J Neurosci* **26**: 1331–1333.

Niswender CM, Johnson KA, Luo Q, Ayala JE, Kim C, Conn PJ *et al* (2008). A novel assay of Gi/o-linked G protein-coupled receptor coupling to potassium channels provides new insights into the pharmacology of the group III metabotropic glutamate receptors. *Mol Pharmacol* **73**: 1213–1224.

O'Brien RJ, Kamboj S, Ehlers MD, Rosen KR, Fischbach GD, Huganir RL (1998). Activity-dependent modulation of synaptic AMPA receptor accumulation. *Neuron* **21**: 1067–1078.

Ohno-Shosaku T, Kim I, Sawada S, Yamamoto C (1996). Presence of the voltage-gated potassium channels sensitive to charybdotoxin in inhibitory presynaptic terminals of cultured rat hippocampal neurons. *Neurosci Lett* **207**: 195–198.

Oliver D, Lien CC, Soom M, Baukrowitz T, Jonas P, Fakler B (2004). Functional conversion between A-type and delayed rectifier K+ channels by membrane lipids. *Science* **304**: 265–270.

Olpe HR, Baudry M, Fagni L, Lynch G (1982). The blocking action of baclofen on excitatory transmission in the rat hippocampal slice. *J Neurosci* **2**: 698–703.

Ouardouz M, Sastry BR (2000). Mechanisms underlying LTP of inhibitory synaptic transmission in the deep cerebellar nuclei. *J Neurophysiol* **84**: 1414–1421.

Paul SM, Syapin PJ, Paugh BA, Moncada V, Skolnick P (1979). Correlation between benzodiazepine receptor occupation and anticonvulsant effects of diazepam. *Nature* **281**: 688–689.

Peretz T, Levin G, Moran O, Thornhill WB, Chikvashvili D, Lotan I (1996). Modulation by protein kinase C activation of rat brain delayed-rectifier K+ channel expressed in Xenopus oocytes. *FEBS Lett* **381**: 71–76.

Pin JP, Van-Vliet BJ, Bockaert J (1988). NMDA- and kainate-evoked GABA release from striatal neurones differentiated in primary culture: differential blocking by phencyclidine. *Neurosci Lett* **87**: 87–92.

Rao A, Craig AM (1997). Activity regulates the synaptic localization of the NMDA receptor in hippocampal neurons. *Neuron* **19**: 801–812.

Rho JM, Szot P, Tempel BL, Schwartzkroin PA (1999). Developmental seizure susceptibility of kv1.1 potassium channel knockout mice. *Dev Neurosci* **21**: 320–327.

Rhodes KJ, Strassle BW, Monaghan MM, Bekele-Arcuri Z, Matos MF, Trimmer JS (1997). Association and colocalization of the Kvbeta1 and Kvbeta2 beta-subunits with Kv1 alpha-subunits

in mammalian brain K+ channel complexes. *J Neurosci* **17**: 8246–8258.
Robertson B (1997). The real life of voltage-gated K+ channels: more than model behaviour. *Trends Pharmacol Sci* **18**: 474–483.
Rudy B, McBain CJ (2001). Kv3 channels: voltage-gated K+ channels designed for high-frequency repetitive firing. *Trends Neurosci* **24**: 517–526.
Sabatini BL, Oertner TG, Svoboda K (2002). The life cycle of Ca(2+) ions in dendritic spines. *Neuron* **33**: 439–452.
Scharfman HE (1994). Paradoxical enhancement by bicuculline of dentate granule cell IPSPs evoked by fimbria stimulation in rat hippocampal slices. *Neurosci Lett* **168**: 29–33.
Schlichter LC, Sakellaropoulos G, Ballyk B, Pennefather PS, Phipps DJ (1996). Properties of K+ and Cl- channels and their involvement in proliferation of rat microglial cells. *Glia* **17**: 225–236.
Schoppa NE, Westbrook GL (2002). AMPA autoreceptors drive correlated spiking in olfactory bulb glomeruli. *Nat Neurosci* **5**: 1194–1202.
Seifert G, Steinhauser C (2001). Ionotropic glutamate receptors in astrocytes. *Prog Brain Res* **132**: 287–299.
Shamotienko OG, Parcej DN, Dolly JO (1997). Subunit combinations defined for K+ channel Kv1 subtypes in synaptic membranes from bovine brain. *Biochemistry* **36**: 8195–8201.
Sheng M, Liao YJ, Jan YN, Jan LY (1993). Presynaptic A-current based on heteromultimeric K+ channels detected in vivo. *Nature* **365**: 72–75.
Sjostrom PJ, Turrigiano GG, Nelson SB (2003). Neocortical LTD via coincident activation of presynaptic NMDA and cannabinoid receptors. *Neuron* **39**: 641–654.
Smart SL, Bosma MM, Tempel BL (1997). Identification of the delayed rectifier potassium channel, Kv1.6, in cultured astrocytes. *Glia* **20**: 127–134.
Smart SL, Lopantsev V, Zhang CL, Robbins CA, Wang H, Chiu SY *et al* (1998). Deletion of the K(V)1.1 potassium channel causes epilepsy in mice. *Neuron* **20**: 809–819.
Smith CC, McMahon LL (2006). Estradiol-induced increase in the magnitude of long-term potentiation is prevented by blocking NR2B-containing receptors. *J Neurosci* **26**: 8517–8522.
Southan AP, Robertson B (1998). Modulation of inhibitory postsynaptic currents (IPSCs) in mouse cerebellar Purkinje and basket cells by snake and scorpion toxin K+ channel blockers. *Br J Pharmacol* **125**: 1375–1381.
Southan AP, Robertson B (2000). Electrophysiological characterization of voltage-gated K(+) currents in cerebellar basket and purkinje cells: Kv1 and Kv3 channel subfamilies are present in basket cell nerve terminals. *J Neurosci* **20**: 114–122.
Staley KJ, Mody I (1992). Shunting of excitatory input to dentate gyrus granule cells by a depolarizing GABAA receptor-mediated postsynaptic conductance. *J Neurophysiol* **68**: 197–212.
Stoppini L, Buchs PA, Muller D (1991). A simple method for organotypic cultures of nervous tissue. *J Neurosci Methods* **37**: 173–182.
Strack S, McNeill RB, Colbran RJ (2000). Mechanism and regulation of calcium/calmodulin-dependent protein kinase II targeting to the NR2B subunit of the N-methyl-D-aspartate receptor. *J Biol Chem* **275**: 23798–23806.
Tang YP, Shimizu E, Dube GR, Rampon C, Kerchner GA, Zhuo M *et al* (1999). Genetic enhancement of learning and memory in mice. *Nature* **401**: 63–69.
Tao Y, Zeng R, Shen B, Jia J, Wang Y (2005). Neuronal transmission stimulates the phosphorylation of Kv1.4 channel at Ser229 through protein kinase A1. *J Neurochem* **94**: 1512–1522.
Telfeian AE, Tseng HC, Baybis M, Crino PB, Dichter MA (2003). Differential expression of GABA and glutamate-receptor subunits and enzymes involved in GABA metabolism between electrophysiologically identified hippocampal CA1 pyramidal cells and interneurons. *Epilepsia* **44**: 143–149.
Trimmer JS, Rhodes KJ (2004). Localization of voltage-gated ion channels in mammalian brain. *Annu Rev Physiol* **66**: 477–519.
van Brederode JF, Rho JM, Cerne R, Tempel BL, Spain WJ (2001). Evidence of altered inhibition in layer V pyramidal neurons from neocortex of Kcna1-null mice. *Neuroscience* **103**: 921–929.
Van Wart A, Trimmer JS, Matthews G (2007). Polarized distribution of ion channels within microdomains of the axon initial segment. *J Comp Neurol* **500**: 339–352.
Vicente R, Escalada A, Villalonga N, Texido L, Roura-Ferrer M, Martin-Satue M *et al* (2006). Association of Kv1.5 and Kv1.3 contributes to the major voltage-dependent K+ channel in macrophages. *J Biol Chem* **281**: 37675–37685.
Vida I, Bartos M, Jonas P (2006). Shunting inhibition improves robustness of gamma oscillations in hippocampal interneuron networks by homogenizing firing rates. *Neuron* **49**: 107–117.
Vogalis F, Ward M, Horowitz B (1995). Suppression of two cloned smooth muscle-derived delayed rectifier potassium channels by cholinergic agonists and phorbol esters. *Mol Pharmacol* **48**: 1015–1023.
Wang XM, Bausch SB (2004). Effects of distinct classes of N-methyl-D-aspartate receptor antagonists on seizures, axonal sprouting and neuronal loss in vitro: suppression by NR2B-selective antagonists. *Neuropharmacology* **47**: 1008–1020.
Wang Y, Bausch SB (2006). In contrast to NR2B-selective antagonists, chronic treatment with NR2A-selective or non-subunit selective antagonists reduced interneuron survival and GAD65/67 expression. *Neurosci Abstr* Program No. 278.16.
Weitlauf C, Honse Y, Auberson YP, Mishina M, Lovinger DM, Winder DG (2005). Activation of NR2A-containing NMDA receptors is not obligatory for NMDA receptor-dependent long-term potentiation. *J Neurosci* **25**: 8386–8390.
Williamson A, Telfeian AE, Spencer DD (1995). Prolonged GABA responses in dentate granule cells in slices isolated from patients with temporal lobe sclerosis. *J Neurophysiol* **74**: 378–387.
Xiang Z, Huguenard JR, Prince DA (2002). Synaptic inhibition of pyramidal cells evoked by different interneuronal subtypes in layer v of rat visual cortex. *J Neurophysiol* **88**: 740–750.
Xie CW, Lewis DV (1995). Endogenous opioids regulate long-term potentiation of synaptic inhibition in the dentate gyrus of rat hippocampus. *J Neurosci* **15**(5 Pt 2): 3788–3795.
Yamakura T, Shimoji K (1999). Subunit- and site-specific pharmacology of the NMDA receptor channel. *Prog Neurobiol* **59**: 279–298.
Yamazaki Y, Hozumi Y, Kaneko K, Li J, Fujii S, Miyakawa H *et al* (2005). Direct evidence for mutual interactions between perineuronal astrocytes and interneurons in the CA1 region of the rat hippocampus. *Neuroscience* **134**: 791–802.
Yang J, Woodhall GL, Jones RS (2006). Tonic facilitation of glutamate release by presynaptic NR2B-containing NMDA receptors is increased in the entorhinal cortex of chronically epileptic rats. *J Neurosci* **26**: 406–410.
Yao H, Zhou K, Yan D, Li M, Wang Y (2009). The Kv2.1 channels mediate neuronal apoptosis induced by excitotoxicity. *J Neurochem* **108**: 909–919.
Zhang CL, Messing A, Chiu SY (1999). Specific alteration of spontaneous GABAergic inhibition in cerebellar purkinje cells in mice lacking the potassium channel Kv1. 1. *J Neurosci* **19**: 2852–2864.
Zhao MG, Toyoda H, Lee YS, Wu LJ, Ko SW, Zhang XH *et al* (2005). Roles of NMDA NR2B subtype receptor in prefrontal long-term potentiation and contextual fear memory. *Neuron* **47**: 859–872.
Zhou M, Baudry M (2006). Developmental changes in NMDA neurotoxicity reflect developmental changes in subunit composition of NMDA receptors. *J Neurosci* **26**: 2956–2963.

Supplementary Information accompanies the paper on the Neuropsychopharmacology website (http://www.nature.com/npp)